High Temperature Vaporization Behavior of Oxides. I. Alkali Metal Binary Oxides

R. H. Lamoreaux and D. L. Hildenbrand

SRI International, Menlo Park, California 94025

In order to assess the high temperature vaporization behavior and equilibrium gas phase compositions of binary alkali metal oxides, the relevant thermodynamic and molecular constant data have been compiled and critically evaluated. Selected values of the Gibbs energy and enthalpy functions of condensed and vapor phases are given in the form of equations valid over wide temperature ranges, along with the standard entropies and enthalpies of formation. These data were used to generate plots of the equilibrium partial pressures of vapor species as functions of temperature for representative conditions ranging from reducing to oxidizing. Maximum vaporization rates have been calculated using the Hertz–Knudsen equation. Literature references are given.

Key words: alkali metal; critically reviewed data; enthalpy increment; enthalpy of formation; Gibbs energy function; high temperature; oxide; partial pressure; vaporization; vaporization rate.

Contents

List of Tables

List of Figures

1. Introduction

1.1. Background

Oxide materials are used or encountered in a wide variety of high temperature applications where vaporization rates and thermodynamic stabilities are often limiting factors. The efficient design and operation of high temperature devices and processes requires reliable information about the stability and volatility of these oxides so that vaporization losses and component lifetimes can be predicted.

Despite continuing research efforts and the use of increasingly sophisticated techniques, there are still many gaps in our knowledge and understanding of the detailed vaporization thermodynamics of metal oxide systems. This puts a premium on critical review of the literature and selection of the necessary thermodynamic data. Even in cases where most of the requisite data are compiled, however, the user still must resort to a significant amount of additional calculations, sometimes unfamiliar, in order to evaluate vapor composition and vaporization behavior for specific environmental conditions. Thus we perceive a definite need for critically evaluated data, presented in a format that gives users ready access to the detailed vaporization chemistry and equilibrium partial pressures of the various species.

Reviews and compilations of data on oxide thermodynamics and vaporization behavior have been done by Brewer,[1] Coughlin,[2] Kelley,[3] Schick,[4] Ackermann and Thorn,[5] Brewer and Rosenblatt,[6,7] Kelley and King,[8] Olette and Ancey-Moret,[9] Wicks and Block,[10] the Bureau of Standards,[11–16] the JANAF group,[17,21] Barin and Knacke,[22] Samsonov *et al.*,[23,24] the IVTAN (High Temperature Institute, State Institute of Applied Chemistry, National Academy of Sciences of the U.S.S.R.) group,[25,26] and Pankratz.[27] Pedley and Marshall[28] have submitted a review of thermodynamic data of gaseous monoxides to this journal. The later reviews are more useful, since much of the relevant data has appeared in the last few years. However, the recent critical reviews by JANAF and IVTAN cover only certain portions of the periodic table and do not include many oxides of interest. This work is the first part of a program sponsored by the Office of Standard Reference Data of the National Bureau of Standards to provide critically reviewed thermodynamic data of oxides, along with overviews of their high temperature data of oxides, along with overviews of their high temperature vaporization phenomena. Participants in the project are Leo Brewer of the University of California at Berkeley, Gerd M. Rosenblatt of the Los Alamos Scientific Laboratory, and the present authors.

1.2. Scope

The present study is intended to serve as a source of critically reviewed thermodynamic data, and to provide an overview of high temperature vaporization phenomena for condensed alkali oxides. Substances considered are condensed phases stable over a portion of the temperature range between 298 and 3000 K and vapor phase species that have been, or under the proper conditions might be, observed in equilibrium with the condensed phases. In the absence of accurate phase boundary data, the solid phases are treated as line compounds. Data are tabulated for liquid phases with compositions identical to the solid phases. The limited amount of thermodynamic data for homogeneous oxide phases of variable composition are cited in the text but were not evaluated. The properties of these phases, and of solutions of oxygen in liquid alkali metals, are beyond the scope of this work, and data necessary for their treatment are for the most part unavailable. The information presented consists of thermodynamic data for the various chemical species involved in the vaporization processes, equilibrium partial pressures of significant vapor species found over condensed oxide phases as functions of temperature and oxygen partial pressure, and maximum vaporization rates calculated from the Hertz–Knudsen equation of classical kinetic theory. Graphs of partial pressures of significant vapor species in equilibrium with condensed phases are provided as a concise reference to vaporization behavior under various conditions of temperature and oxygen potential.

1.3. Literature Reviewed

A thorough search was made in Chemical Abstracts and in the Bulletin of Chemical Thermodynamics and Thermochemistry for entries related to the substances under consideration. The literature review encompassed publications up to about December 1982. When an adequate review of earlier work on a subject is available, reference is given to the review only, except when specific references are desirable.

2. Thermodynamic Properties

2.1. Discussion

a. Evaluation of Data

The methods of data evaluation used in the present work are similar to those used for the JANAF tables[17] and need not be repeated in detail. In addition to consistency of data within a given source and general assessments of experimental methods, criteria for data evaluation included the degree of agreement of second- and third-law reaction enthalpies evaluated from equilibrium data. For gaseous alkali metal monoxides, the Rittner ionic model[29,30] was used as an aid in data evaluation. Data from original sources were recalculated, when necessary, using selected values of auxiliary data. CODATA[31] values were used when available. Selected thermodynamic data derived from experimental information are consistent with the original observations within experimental uncertainty.

The mathematical procedures used to process thermodynamic data have been discussed by JANAF,[17] among others. Data for substances undergoing transitions between solid phase forms or between solid and liquid phases were treated by using data for the lower temperature form below the normal transition temperature, taking the enthalpy and entropy of transition into account at the transition temperature, and using data for the higher temperature form above the transition temperature. The Gibbs energy functions of condensed phases calculated by this procedure are consistent with the enthalpies of formation of the condensed phase stable at 298.15 K and 1.013 25 bar.

b. Symbols

The thermodynamic symbols used in the present work are

$\Delta_f H^\circ_{298}/R$	The standard molar enthalpy of formation at 298.15 K divided by the molar gas constant
$(H^\circ_{298} - H^\circ_0)/R$	The molar enthalpy increment between 0 and 298.15 K divided by the molar gas constant
$-(G^\circ_T - H^\circ_{298})/RT$	The molar Gibbs energy function divided by the molar gas constant
$(H^\circ_T - H^\circ_{298})/R$	The molar enthalpy increment between 298.15 and T K divided by the molar gas constant
S°_T/R	The standard molar entropy at T K divided by the molar gas constant
$T_{trs}, \Delta_{trs}H^\circ/R$	Solid-phase transition temperature and molar enthalpy of transition divided by the molar gas constant
$T_{fus}, \Delta_{fus}H^\circ/R$	Melting temperature and molar enthalpy of fusion divided by the molar gas constant.

c. Units

Following the suggestion of Pitzer and Brewer,[32] thermodynamic quantities are expressed in dimensionless units, e.g., S°/R, G°/RT, or in Kelvin units, e.g., $\Delta H^\circ/R$, $\Delta G^\circ/R$. The symbols K and kK, where 1 kK = 10^3 K, are used to represent Kelvin units. Values of R used in the present work are 1.987 19 cal/mol K and 8.3144 J/mol K. The temperature scale is nominally the 1968 International Practical Temperature Scale (IPTS) for measured quantities and the thermodynamic temperature scale for estimated quantities and calculated gaseous quantities. If conversion to the 1948 IPTS is desired, subtract 1 K between 1015 and 1380 K and 2 K between 1381 and 1926 K, for an accuracy within 1 K. The atomic weights are from the 1975 Report of the Commission on Atomic Weights, Inorganic Division of IUPAC.[33]

Molecular constants cited in the text are internuclear distances r in cm, vibrational fundamentals ω in cm^{-1}, the molecular symmetry number σ, electronic state quantum weights g_i, and excited electronic state term values T_e in cm^{-1}. A more thorough discussion of these quantities and their use in calculating thermodynamic functions has been given in JANAF.[17]

Table 1. Alkali metal oxides melting above 300 K, their melting temperatures, and enthalpies of fusion.[a]

	T_m (K)	$\Delta_{fus}H/R$ (kK)
Li_2O	1711 ± 5	6.5 ± 1.0
Li_2O_2	1250 ± 250[b]	5.0 ± 2.0[b]
NaO_2	825 ± 10	3.3 ± 1.0
Na_2O	1405 ± 100[c]	5.7 ± 0.5[c]
Na_2O_2	948 ± 150[c]	3.9 ± 0.7
KO_2	865 ± 80[c]	1.6 ± 0.7[c]
K_2O	1190 ± 50	4.8 ± 1.0
K_2O_2	763 ± 100[c]	3.1 ± 1.0
RbO_2	685 ± 100[c]	2.7 ± 0.6
Rb_2O	900 ± 50	3.7 ± 1.0
Rb_2O_2	843 ± 100[c]	3.4 ± 0.7
CsO_2	723 ± 50[c]	3.0 ± 0.5
CsO_3	343 ± 70[d]	
Cs_2O	768 ± 5	3.1 ± 0.5
Cs_2O_2	863 ± 100[c]	3.5 ± 0.5
Cs_3O	437 ± 4[e]	

[a] See table 5 for references.

[b] Estimated

[c] Uncertainty estimated (this work).

[d] Peritectic decomposition to CsO_2 and liquid.

[e] Peritectic decomposition to Cs_2O and liquid.

Table 2. Gibbs energy functions of substances encountered in the high temperature vaporization of alkali metal oxides.

	$-(G^\circ_T-H^\circ_{298})/RT = A + BT + CT^2 + DT^3$				
	A	10^3B	10^6C	10^9D	T Range (K)
O(g)	19.92	-4.808	11.711	-6.412	298 - 800
	18.23	3.200	-0.891	0.122	800 -1600
	18.54	2.639	-0.551	0.053	1600 -3000
O_2(g)	25.46	-6.723	16.189	-8.707	298 - 800
	23.11	4.240	-0.889	0.088	800 -1600
	23.35	3.886	-0.726	0.066	1600 -3000
O_3(g)	18.68	26.852	-28.145	13.976	298 - 600
	21.20	14.143	-6.413	1.381	600 -1400
	23.86	8.201	-1.892	0.214	1400 -3000
Li(s)	3.98	-3.544	6.775	0.000	298 -453
Li(l)	1.42	6.096	-2.229	0.386	453 -1500
	3.33	2.796	-0.300	0.000	1500 -3000
Li(g)	17.23	-4.681	11.351	-6.194	298 - 800
	15.64	2.942	-0.713	0.080	800 -3000
LiO(g)	26.79	-11.266	27.053	-16.660	298 - 600
	23.96	3.847	-0.170	-0.163	600 -1400
	23.86	4.403	-0.857	0.079	1400 -3000
LiO_2(g)	31.29	-15.850	37.839	-23.079	298 - 600
	27.24	5.515	-0.227	-0.225	600 -1400
	27.08	6.366	-1.227	0.115	1400 -3000
Li_2(g)	25.25	-12.740	30.728	-19.081	298 - 600
	22.02	4.591	-0.578	-0.071	600 -1400
	22.14	4.671	-0.910	0.081	1400 -3000
Li_2O(s)	7.22	-21.201	50.163	-30.238	298 - 600
	2.00	6.391	0.899	-0.631	600 -1300
	6.98	-2.441	5.633	-1.311	1300 -1711
Li_2O(l)	-8.27	18.200	-4.168	0.410	1711 -3000
Li_2O(g)	29.78	-17.904	42.895	-26.299	298 - 600
	25.18	6.391	-0.501	-0.189	600 -1400
	25.11	7.070	-1.399	0.131	1400 -3000
Li_2O_2(s)	10.18	-26.989	63.832	-38.277	298 - 600
	3.56	7.970	1.514	-0.867	600 -1250
Li_2O_2(l)	-6.65	23.805	-6.842	0.910	1250 -2000
Li_2O_2(g)	33.79	-22.112	52.593	-31.942	298 - 600
	28.15	7.556	-0.101	-0.380	600 -1400
	27.76	9.099	-1.769	0.164	1400 -3000
Li_3(g)	35.23	-19.938	48.156	-30.024	298 - 600
	30.14	7.376	-1.212	-0.022	600 -1400
	30.43	7.247	-1.506	0.145	1400 -3000
Li_3O(g)	35.73	-24.797	59.413	-36.522	298 - 600
	29.44	8.625	-0.554	-0.314	600 -1400
	29.42	9.505	-1.852	0.173	1400 -3000
Na(s)	7.27	-7.591	12.955	0.000	298 - 371
Na(l)	4.78	3.249	2.713	-2.360	371 - 700
	4.10	6.542	-2.625	0.509	700 -1400
	5.29	4.045	-0.853	0.083	1400 -3000
Na(g)	19.03	-4.681	11.351	-6.194	298 - 800
	17.44	2.935	-0.708	0.079	800 -3000
NaO(g)	29.00	-12.251	29.466	-18.185	298 - 600
	25.95	4.104	-0.075	-0.252	600 -1200
	25.75	4.932	-1.060	0.106	1200 -3000
NaO_2(s)	15.92	-16.637	39.727	-20.900	298 - 825
NaO_2(l)	4.82	19.292	-5.267	0.623	825 -3000
NaO_2(g)	32.89	-17.038	40.869	-25.116	298 - 600
	28.65	5.644	0.013	-0.377	600 -1200
	28.33	6.905	-1.442	0.142	1200 -3000
Na_2(g)	29.30	-13.120	31.694	-19.719	298 - 600
	25.96	4.770	-0.653	-0.056	600 -1400
	25.93	5.111	-1.101	0.103	1400 -3000

Table 2. Gibbs energy functions of substances encountered in the high temperature vaporization of alkali metal oxides.--Continued

	$-(G^\circ_T-H^\circ_{298})/RT = A + BT + CT^2 + DT^3$				
	A	10^3B	10^6C	10^9D	T Range (K)
Na_2O(s)	12.07	-24.530	58.798	-36.029	298 - 600
	5.85	8.562	-0.633	-0.103	600 -1300
	5.74	8.638	-0.764	0.000	1300 -1405
Na_2O(l)	7.67	6.193	0.000	0.000	1405 -3000
Na_2O(g)	33.81	-19.835	47.718	-29.514	298 - 600
	28.82	6.843	-0.428	-0.304	600 -1200
	28.65	7.801	-1.673	0.168	1200 -3000
Na_2O_2(s)	14.11	-22.460	53.337	-28.544	298 - 785
	7.25	10.565	0.000	0.000	785 - 948
Na_2O_2(l)	9.33	8.368	0.000	0.000	948 -3000
Na_2O_2(g)	38.25	-25.730	61.721	-38.044	298 - 600
	31.80	8.719	-0.327	-0.461	600 -1200
	31.47	10.223	-2.170	0.216	1200 -3000
K(s)	8.55	-3.293	-3.967	21.487	298 - 336
K(l)	8.07	-7.660	27.588	-21.265	336 - 500
	5.88	6.301	-2.422	0.463	500 -1300
	6.74	4.407	-1.018	0.113	1300 -3000
K(g)	20.16	-7.220	17.477	-10.913	298 - 600
	18.32	2.665	-0.428	-0.016	600 -1400
	18.43	2.624	-0.553	0.054	1400 -3000
KO(g)	30.30	-13.720	33.313	-20.900	298 - 600
	26.77	5.249	-1.084	0.057	600 -1400
	27.11	4.846	-1.027	0.100	400 -3000
KO_2(s)	18.26	-28.382	67.924	-41.676	298 - 600
	11.55	8.027	1.568	-1.154	600 - 865
KO_2(l)	7.69	16.211	-4.146	0.478	865 -3000
KO_2(g)	33.98	-17.218	41.356	-25.457	298 - 600
	29.83	5.207	0.578	-0.598	600 -1200
	29.40	6.937	-1.453	0.144	1200 -3000
K_2(g)	31.67	-13.248	32.007	-19.914	298 - 600
	28.28	4.858	-0.654	-0.095	600 -1400
	28.29	5.247	-1.247	0.127	1400 -3000
K_2O(s)	14.68	-27.005	64.596	-39.642	298 - 600
	8.73	5.772	4.132	-2.363	600 - 890
	2.42	26.192	-17.967	5.636	890 -1190
K_2O(l)	0.80	18.889	-4.532	0.467	1190 -3000
K_2O(g)	36.52	-19.066	45.948	-28.502	298 - 600
	31.63	7.039	-1.027	-0.062	600 -1400
	31.83	7.112	-1.465	0.141	1400 -3000
K_2O_2(s)	16.08	-24.847	59.193	-31.877	298 - 763
K_2O_2(l)	1.90	25.223	-7.055	0.859	763 -3000
K_2O_2(g)	41.01	-27.084	65.212	-40.422	298 - 600
	34.06	9.978	-1.428	-0.095	600 -1400
	34.32	10.122	-2.079	0.199	1400 -3000
Rb(s)	9.15	0.278	0.000	0.000	298 - 313
Rb(l)	8.93	-2.497	14.303	-10.022	313 - 600
	7.28	6.671	-2.722	0.536	600 -1400
	8.49	4.095	-0.872	0.087	1400 -3000
Rb(g)	21.33	-7.220	17.477	-10.913	298 - 600
	19.48	2.721	-0.492	0.008	600 -1400
	19.61	2.617	-0.551	0.054	1400 -3000
RbO(g)	31.31	-15.061	36.458	-22.913	298 - 600
	27.44	5.774	-1.306	0.092	600 -1400
	27.88	5.169	-1.127	0.112	1400 -3000
RbO_2(s)	18.55	-23.671	56.381	-32.530	298 -685
RbO_2(l)	6.64	20.954	-6.185	0.777	685 -3000

Table 2. Gibbs energy functions of substances encountered in the high temperature vaporization of alkali metal oxides.--Continued

$-(G^\circ_T-H^\circ_{298})/RT = A + BT + CT^2 + DT^3$

	A	10^3B	10^6C	10^9D	T Range (K)
RbO_2(g)	35.49	-17.470	41.958	-25.875	298 - 600
	31.01	6.308	-0.689	-0.122	600 -1400
	31.05	6.699	-1.336	0.126	1400 -3000
Rb_2(g)	34.09	-13.042	31.551	-19.709	298 - 600
	30.75	4.882	-0.870	0.008	600 -1400
	30.98	4.706	-0.984	0.096	1400 -3000
Rb_2O(s)	18.49	-25.515	60.654	-35.906	298 - 675
	11.84	9.461	-0.805	0.000	675 - 750
	13.01	6.413	1.174	0.000	750 - 810
	22.56	-27.259	40.596	-15.312	810 - 900
Rb_2O(l)	4.60	21.797	-6.188	0.744	900 -3000
Rb_2O(g)	38.69	-19.261	46.426	-28.837	298 - 600
	33.76	7.098	-1.065	-0.052	600 -1400
	33.98	7.121	-1.466	0.141	1400 -3000
Rb_2O_2(s)	18.54	-22.449	53.321	-27.871	298 - 843
Rb_2O_2(l)	4.69	24.083	-6.542	0.782	843 -3000
Rb_2O_2(g)	43.19	-27.341	65.845	-40.844	298 - 600
	36.17	10.088	-1.495	-0.079	600 -1400
	36.49	10.138	-2.081	0.199	1400 -3000
Cs(s)	10.20	0.143	0.000	0.000	290 - 302
Cs(l)	10.00	-2.498	13.761	-9.509	301 - 600
	8.47	6.048	-2.139	0.371	600 -1400
	9.34	4.284	-0.938	0.095	1400 -3000
Cs(g)	22.00	-7.220	17.477	-10.913	298 - 600
	20.14	2.721	-0.492	0.008	600 -1400
	20.26	2.644	-0.566	0.057	1400 -3000
CsO(g)	31.75	-14.342	34.392	-21.217	298 - 600
	27.99	5.474	-0.899	-0.034	600 -1400
	28.23	5.389	-1.175	0.116	1400 -3000
CsO_2(s)	19.16	-19.641	47.344	-26.434	298 - 723
CsO_2(l)	8.20	19.410	-5.268	0.615	723 -3000
CsO_2(g)	36.29	-17.557	42.187	-26.044	298 - 600
	31.81	6.285	-0.658	-0.133	600 -1400
	31.82	6.735	-1.353	0.128	1400 -3000
Cs_2(g)	35.14	-8.705	21.922	-12.719	298 - 600
	32.38	4.955	-0.822	-0.002	600 -1400
	32.50	4.043	-0.905	0.097	1400 -3000
Cs_2O(s)	19.86	-18.388	44.069	-23.923	298 - 768
Cs_2O(l)	11.10	14.255	-1.953	0.000	768 -3000
Cs_2O(g)	40.61	-19.222	46.327	-28.754	298 - 600
	35.68	7.100	-1.063	-0.053	600 -1400
	35.89	7.136	-1.427	0.142	1400 -3000
Cs_2O_2(s)	19.88	-21.301	50.979	-26.536	298 - 863
Cs_2O_2(l)	6.32	23.533	-6.310	0.748	863 -3000
Cs_2O_2(g)	44.36	-27.134	65.374	-40.513	298 - 600
	37.38	10.047	-1.461	-0.089	600 -1400
	37.67	10.151	-2.088	0.200	1400 -3000

Table 3. Enthalpy increment above 298.15 K of substances encountered in the high temperature vaporization of alkali metal oxides. (*Units* = kK)

$(H^\circ_T-H^\circ_{298})/R = a + bT + cT^2 + dT^3$

	a	10^3b	10^6c	10^9d	T Range (K)
O(g)	-0.81	2.849	-0.460	0.220	298 - 800
	-0.74	2.550	-0.022	0.004	800 -3000
O_2(g)	-1.00	3.201	0.517	0.027	298 - 800
	-1.21	3.665	0.301	-0.026	800 -3000
O_3(g)	-1.11	2.540	4.423	-1.655	298 - 800
	-1.79	5.136	1.061	-0.178	800 -1400
	-3.41	8.872	-1.787	0.540	1400 -3000
Li(s)	-0.71	1.825	1.880	0.000	298 - 454
Li(l)	-0.83	3.893	-0.382	0.109	454 -1500
	-0.66	3.452	0.000	0.000	1500 -3000
Li(g)	-0.75	2.505	-0.011	0.007	298 -1000
	-0.79	2.598	-0.069	0.016	1000 -3000
LiO(g)	-1.03	3.102	1.356	-0.421	298 -1000
	-1.49	4.346	0.176	-0.029	1000 -3000
LiO_2(g)	-1.32	3.523	3.448	-1.277	298 -1000
	-2.03	6.054	0.382	-0.036	1000 -3000
Li_2(g)	-1.26	4.064	0.573	-0.173	298 -1000
	-1.05	3.626	0.811	-0.180	1000 -2000
	-2.84	6.172	-0.395	0.009	2000 -3000
Li_2O(s)	-1.50	3.113	7.280	-2.706	298 - 800
	-2.20	6.271	2.475	-0.285	800 -1300
	43.02	-63.456	28.986	0.000	1300 -1400
	-68.98	122.314	-64.562	12.854	1400 -1711
Li_2O(l)	1.56	12.077	0.000	0.000	1711 -3000
Li_2O(g)	-1.59	4.555	2.933	-1.090	298 -1000
	-2.32	6.959	0.195	-0.025	1000 -3000
Li_2O_2(s)	-1.85	3.431	10.570	-4.095	298 - 600
	-2.59	7.212	4.044	-0.299	600 -1250
Li_2O_2(l)	-2.97	16.103	0.000	0.000	1250 -2000
Li_2O_2(g)	-1.72	4.185	6.036	-2.307	298 -1000
	-3.17	9.068	0.336	-0.043	1000 -3000
Li_3(g)	-2.00	6.576	0.497	-0.205	298 -1000
	-2.10	6.951	0.020	-0.003	1000 -3000
Li_3O(g)	-2.20	6.372	3.833	-1.467	298 -1000
	-2.73	8.650	0.712	-0.092	1000 -3000
Na(s)	-0.73	1.534	3.025	0.000	298 - 371
Na(l)	-1.00	4.704	-1.519	0.648	371 - 700
	-0.87	4.189	-0.796	0.295	700 -1400
	-0.80	3.417	0.167	-0.024	1400 -3000
Na(g)	-0.75	2.505	-0.011	0.007	298 -1000
	-0.77	2.548	-0.033	0.007	1000 -3000
NaO(g)	-1.15	3.502	1.334	-0.501	298 -1000
	-1.57	4.806	-0.050	0.002	1000 -3000
NaO_2(s)	-2.37	7.200	2.470	-0.005	298 - 825
NaO_2(l)	-1.86	12.581	0.000	0.000	825 -3000
NaO_2(g)	-1.52	4.341	2.849	-1.184	298 - 800
	-2.07	6.368	0.255	-0.036	800 -3000
Na_2(g)	-1.33	4.373	0.260	-0.021	298 -1000
	-1.49	4.535	0.440	-0.196	1000 -2000
	-3.20	7.463	-1.237	0.124	2000 -3000

Table 3. Enthalpy increment above 298.15 K of substances encountered in the high temperature vaporization of alkali metal oxides. (Units = kK) --Continued

	$(H^\circ_T-H^\circ_{298})/R = a + bT + cT^2 + dT^3$				
	a	10^3b	10^6c	10^9d	T Range (K)
$Na_2O(s)$	-2.28	6.973	2.245	-0.008	298 -1000
	-16.13	50.726	-45.680	16.019	1000 -1300
	-9.12	15.618	0.000	0.000	1300 -1405
$Na_2O(l)$	0.89	12.581	0.000	0.000	1405 -3000
$Na_2O(g)$	-1.87	5.774	1.934	-0.776	298 -1000
	-2.30	7.298	0.072	-0.009	1000 -3000
$Na_2O_2(s)$	-2.70	7.093	7.379	-2.661	298 - 785
	-3.91	13.661	0.000	0.000	785 - 948
$Na_2O_2(l)$	-2.90	16.774	0.000	0.000	948 -3000
$Na_2O_2(g)$	-2.27	6.470	4.420	-2.026	298 - 800
	-3.02	9.508	0.202	-0.029	800 -3000
K(s)	-5.31	44.899	-134.115	145.167	298 - 336
K(l)	-0.97	4.470	-1.145	0.491	336 -1000
	-0.44	2.917	0.366	-0.001	1000 -3000
K(g)	-0.75	2.505	-0.011	0.007	298 -1000
	-0.83	2.694	-0.139	0.032	1000 -3000
KO(g)	-1.49	5.177	-0.737	0.287	298 -1000
	-1.32	4.586	-0.033	0.004	1000 -3000
$KO_2(s)$	-2.45	6.796	5.390	-2.202	298 - 865
$KO_2(l)$	-3.22	12.581	0.000	0.000	865 -3000
$KO_2(g)$	-1.59	4.760	2.150	-0.783	298 -1000
	-2.14	6.537	0.166	-0.021	1000 -3000
$K_2(g)$	-1.31	4.189	0.807	-0.430	298 -1000
	-2.27	6.708	-1.357	0.173	1000 -3000
$K_2O(s)$	-2.29	6.249	5.508	-2.362	298 - 890
	-145.88	460.411	-473.284	165.926	890 -1070
	-25.75	45.078	-12.511	0.000	1070 -1190
$K_2O(l)$	0.02	12.581	0.000	0.000	1190 -3000
$K_2O(g)$	-1.85	5.865	1.296	-0.525	298 -1000
	-2.13	6.876	0.045	-0.006	1000 -3000
$K_2O_2(s)$	-3.35	10.417	2.473	1.023	298 - 763
$K_2O_2(l)$	-3.19	16.772	0.000	0.000	763 -3000
$K_2O_2(g)$	-2.50	7.434	3.773	-2.062	298 - 600
	-2.88	9.360	0.444	-0.113	600 -1400
	-3.09	9.859	0.046	-0.006	1400 -3000
Rb(s)	-1.14	3.820	0.000	0.000	298 - 313
Rb(l)	-1.11	5.039	-1.745	0.648	313 - 800
	-1.02	4.744	-1.403	0.514	800 -1400
	-0.72	3.387	0.132	0.001	1400 -3000
Rb(g)	-0.75	2.505	-0.011	0.007	298 -1000
	-0.84	2.713	-0.154	0.036	1000 -3000
RbO(g)	-1.56	5.330	-0.318	-0.026	298 -1000
	-1.33	4.869	-0.136	0.018	1000 -3000

Table 3. Enthalpy increment above 298.15 K of substances encountered in the high temperature vaporization of alkali metal oxides. (Units = kK) --Continued

	$(H^\circ_T-H^\circ_{298})/R = a + bT + cT^2 + dT^3$				
	a	10^3b	10^6c	10^9d	T Range (K)
$RbO_2(s)$	-2.38	6.225	6.930	-3.450	298 - 685
$RbO_2(l)$	-1.87	12.581	0.000	0.000	685 -3000
$RbO_2(g)$	-1.62	4.900	1.984	-0.713	298 -1000
	-2.13	6.542	0.165	-0.021	1000 -3000
$Rb_2(g)$	-1.34	4.495	0.002	0.000	298 -1000
	-1.38	4.571	-0.050	0.011	1000 -3000
$Rb_2O(s)$	-2.29	5.844	7.205	-3.662	298 - 675
	-1.70	5.629	3.757	0.000	675 - 750
	42.92	-111.056	80.013	0.000	750 - 810
	-21.15	47.127	-17.613	0.000	810 - 900
$Rb_2O(l)$	-0.65	12.581	0.000	0.000	900 -3000
$Rb_2O(g)$	-1.87	5.963	1.190	-0.484	298 -1000
	-2.12	6.885	0.042	-0.006	1000 -3000
$Rb_2O_2(s)$	-2.84	7.387	8.193	-3.258	298 - 843
$Rb_2O_2(l)$	-3.44	16.774	-0.001	0.000	843 -3000
$Rb_2O_2(g)$	-2.63	8.322	1.958	-0.805	298 -1000
	-3.04	9.827	0.037	-0.008	1000 -3000
Cs(s)	-1.15	3.860	0.000	0.000	298 - 302
Cs(l)	-0.95	4.187	-0.652	0.293	302 -1000
	-0.83	3.719	-0.026	0.019	1000 -3000
Cs(g)	-0.75	2.505	-0.011	0.007	298 -1000
	-0.78	2.597	-0.087	0.026	1000 -2000
	-1.58	3.809	-0.708	0.133	2000 -3000
CsO(g)	-1.13	2.627	4.790	-2.958	298 - 600
	-1.78	5.832	-0.588	0.094	600 -1400
	-1.45	5.236	-0.235	0.027	1400 -3000
$CsO_2(s)$	-2.78	9.206	0.187	0.687	298 - 723
$CsO_2(l)$	-1.89	12.581	0.000	0.000	723 -3000
$CsO_2(g)$	-1.60	4.739	2.430	-1.066	298 - 600
	-1.82	5.758	0.820	-0.202	600 -1400
	-2.21	6.668	0.106	-0.012	1400 -3000
$Cs_2(g)$	-1.35	4.447	0.257	-0.071	298 - 600
	-1.35	4.497	0.149	0.001	600 -1400
	-1.50	4.797	-0.067	0.054	1400 -3000
$Cs_2O(s)$	-2.54	7.925	2.036	-0.010	298 - 768
$Cs_2O(l)$	-1.80	12.581	0.000	0.000	768 -3000
$Cs_2O(g)$	-1.83	5.673	1.889	-1.008	298 - 600
	-2.02	6.611	0.279	-0.073	600 -1400
	-2.14	6.907	0.032	-0.004	1400 -3000
$Cs_2O_2(s)$	-3.19	9.820	3.178	-0.354	298 - 863
$Cs_2O_2(l)$	-3.60	16.771	0.001	-0.000	863 -3000
$Cs_2O_2(g)$	-2.55	7.747	3.261	-1.755	298 - 600
	-2.88	9.403	0.422	-0.108	600 -1400
	-3.07	9.863	0.047	-0.006	1400 -3000

Table 4. Values of $\Delta_f H^\circ_{298}/R$, S°_{298}/R, and $(H^\circ_{298}-H^\circ_0)/R$ of substances encountered in the high temperature vaporization of alkali metal oxides.

	$\Delta_f H^\circ_{298}/R$ (kK)	S°_{298}/R	$(H^\circ_{298}-H^\circ_0)/R$ (kK)
O(g)	29.97 ± 0.01	19.36 ± 0.00	0.81
O_2(g)	0.00 ± 0.00	24.66 ± 0.01	1.04
O_3(g)	17.06 ± 0.24	28.73 ± 0.01	1.25
Li(s)	0.00 ± 0.00	3.50 ± 0.02	0.56
Li(g)	19.17 ± 0.05	16.68 ± 0.00	0.75
LiO(g)	8.30 ± 0.50	25.39 ± 0.30	1.06
LiO_2(g)	9.30 ± 3.50[a]	29.32 ± 0.75	1.31
Li_2(g)	25.85 ± 0.15	23.68 ± 0.01	1.16
Li_2O(s)	-71.91 ± 0.04	4.56 ± 0.02	0.87
Li_2O(g)	-20.78 ± 0.45	27.56 ± 0.75	1.50
Li_2O_2(s)	-76.30 ± 1.00	6.79 ± 0.50	
Li_2O_2(g)	-35.00 ± 3.00	31.03 ± 1.00	1.63
Li_3(g)	38.25 ± 4.00	32.77 ± 1.00	1.75
Li_3O(g)	-28.14 ± 5.00	32.65 ± 1.00	1.88
Na(s)	0.00 ± 0.00	6.17 ± 0.02	0.78
Na(g)	12.88 ± 0.05	18.47 ± 0.00	0.75
NaO(g)	12.58 ± 0.50	27.48 ± 0.30	1.12
NaO_2(s)	-31.35 ± 0.35	13.94 ± 0.15	2.21
NaO_2(g)	-1.01 ± 0.25[a]	30.78 ± 0.75	1.42
Na_2(g)	17.17 ± 0.15	27.68 ± 0.01	1.25
Na_2O(s)	-50.17 ± 0.50	9.03 ± 0.02	1.49
Na_2O(g)	-3.82 ± 1.00	31.35 ± 0.75	1.64
Na_2O_2(s)	-61.65 ± 0.60	11.40 ± 0.15	1.89
Na_2O_2(g)	-10.00 ± 4.00	35.05 ± 1.00	1.91
K(s)	0.00 ± 0.00	7.78 ± 0.02	0.85
K(g)	10.73 ± 0.03	19.27 ± 0.00	0.75
KO(g)	7.20 ± 0.50	28.61 ± 0.30	1.28
KO_2(s)	-34.22 ± 0.25	14.73 ± 0.50	2.00
KO_2(g)	0.60 ± 2.50[a]	31.84 ± 0.75	1.46

Table 4. Values of $\Delta_f H^\circ_{298}/R$, S°_{298}/R, and $(H^\circ_{298}-H^\circ_0)/R$ of substances encountered in the high temperature vaporization of alkali metal oxides.--Cont.

	$\Delta_f H^\circ_{298}/R$ (kK)	S°_{298}/R	$(H^\circ_{298}-H^\circ_0)/R$ (kK)
K_2(g)	15.30 ± 0.50	30.03 ± 0.01	1.29
K_2O(s)	-43.58 ± 0.25	11.32 ± 0.75	
K_2O(g)	-7.05 ± 0.26	34.17 ± 0.75	1.64
K_2O_2(s)	-59.43 ± 0.50	13.09 ± 0.75	
K_2O_2(g)	-20.00 ± 1.00	37.66 ± 1.00	2.10
Rb(s)	0.00 ± 0.00	9.23 ± 0.04	0.90
Rb(g)	9.73 ± 0.03	20.44 ± 0.00	0.75
RbO(g)	7.10 ± 0.50	29.45 ± 0.30	1.25
RbO_2(s)	-33.57 ± 0.30	15.65 ± 0.08	2.02
RbO_2(g)	4.50 ± 2.50[a]	33.32 ± 0.75	1.49
Rb_2O(s)	-40.76 ± 1.56	15.32 ± 0.75	0.00
Rb_2(g)	13.89 ± 0.30	32.48 ± 0.30	1.30
Rb_2O(g)	-8.05 ± 2.50	36.31 ± 0.75	1.66
Rb_2O_2(s)	-57.57 ± 2.40	15.85 ± 0.75	
Rb_2O_2(g)	-19.10 ± 4.00	39.81 ± 1.00	2.14
Cs(s)	0.00 ± 0.00	10.25 ± 0.05	0.93
Cs(g)	9.22 ± 0.25	21.11 ± 0.00	0.75
CsO(g)	4.90 ± 0.50	29.96 ± 0.30	1.19
CsO_2(s)	-34.42 ± 0.25	16.81 ± 0.75	
CsO_2(g)	1.00 ± 2.50[a]	34.11 ± 0.75	1.51
Cs_2(g)	13.74 ± 0.51	34.15 ± 0.10	1.33
Cs_2O(s)	-41.61 ± 0.14	17.66 ± 0.05	2.13
Cs_2O(g)	-19.10 ± 3.00	38.23 ± 1.00	1.66
Cs_2O_2(s)	-59.88 ± 1.26	17.36 ± 0.75	
Cs_2O_2(g)	-30.20 ± 3.00	41.01 ± 1.00	2.14

[a] Estimated lower limit (see text).

Table 5. Sources of data in tables 1 through 4.

	$-(G^\circ_T-H^\circ_{298})/T$, $(H^\circ_T-H^\circ_{298})$	$\Delta_f H^\circ_{298}$	S°_{298}	$(H^\circ_{298}-H^\circ_0)$	T_{fus}, $\Delta_{fus}H$
O(g)	17	17[a],31	17[a],31	17[a],31	
O_2(g)	17	17[a],31	17[a],31	17[a],31	
O_3(g)	25	25	25	25	
Li(s,l)	48[b]	48,31	48,31	48	
Li(g)	17	48	17	17	
LiO(g)	c	105	c	c	
LiO_2(g)	c	d,e	c	c	
Li_2(g)	77[d]	78	77[d]	77[d]	
Li_2O(s,l)	17[b]	106	17	17	46[h]
Li_2O(g)	c	d	c	c	
Li_2O_2(s,l)	17[b]	17	d,e		e
Li_2O_2(g)	c	d	c	c	
Li_3(g)	c	95[f]	c	c	
Li_3O(g)	c	d	c	c	
Na(s,l)	b,d		48,31	48,31	48
Na(g)	17	48	17	17	
NaO(g)	c	76	c	c	
NaO_2(s,l)	17[b]	17	17	17	17[h]
NaO_2(g)	c	d,e	c	c	
Na_2(g)	77	74[f]	77	77	
Na_2O(s,l)	50[b,d]	d	17	17	53
Na_2O(g)	c	d	c	c	
Na_2O_2(s,l)	17[b]	17[i]	17	17	17h
Na_2O_2(g)	c	d,e	c	c	
K(s,l)	48[b]		48,31	48,31	48
K(g)	17	48	17	17	
KO(g)	c	107[d]	c	c	
KO_2(s,l)	18[b]	36[i]	18	18	57
KO_2(g)	c	d,e	c	c	
K_2(g)	77	74[f]	77	77	
K_2O(s,l)	d,e	17[d]	d,e		d,e,h
K_2O(g)	c	d	c	c	
K_2O_2(s,l)	17[b]	d	d,e		17[h]
K_2O_2(g)	c	d	c	c	
Rb(s,l)	48[b]		31,48	31,48	48
Rb(g)	108	48	108	108	108
RbO(g)	c	d,e	c	c	
RbO_2(s,l)	66[b]	36[i]	66	66	67[h]
RbO_2(g)	c	d,e	c	c	
Rb_2(g)	c,d	74[f]	c,d	c,d	
Rb_2O(s,l)	d,e	16	d,e		d,e,h
Rb_2O(g)	c	82[g]	c	c	
Rb_2O_2(s,l)	d,e	68[g]	d,e	d,e	67[h]
Rb_2O_2(g)	c	d,e	c	c	
Cs(s,l)	17[b]		17,31	17,31	109
Cs(g)	17	17	17	17	
CsO(g)	c	d,e	c	c	
CsO_2(s,l)	e	36[i]	e		70[h]
CsO_2(g)	c	d,e	c	c	
Cs_2(g)	17[d]	74[f]	17[d]	17[d]	
Cs_2O(s,l)	72[b]	110	72	72	111[h]
Cs_2O(g)	c	d,e	c	c	
Cs_2O_2(s,l)	d,e	73[d,g]	d,e		70[h]
Cs_2O_2(g)	c	d,e	c	c	

Table 5. Sources of data in tables 1 through 4.--Continued

[a] March 31, 1977 supplement.

[b] Some values were estimated; see text.

[c] Calculated from molecular constants; see text.

[d] See text.

[e] Estimated.

[f] The enthalpy of formation was calculated from the dissociation energy.

[g] Data from the cited source were used to calculate value.

[h] The enthalpy of fusion was estimated.

[i] Recalculated using CODATA[31] values of auxiliary data.

2.2. Selected Thermodynamic Data

Selected values of the thermochemical properties of substances encountered in the high temperature vaporization of alkali metal oxides are shown in Tables 1–4. Where possible, sources of the data in Tables 1–4 are given in Table 5. Table 1 lists the solid high temperature alkali metal oxide phases and their melting or dissociation temperatures. Table 2 presents Gibbs energy functions of oxygen and alkali oxide species fit to the equation

$$-(G^\circ_T - H^\circ_{298})/RT = A + BT + CT^2 + DT^3. \quad (1)$$

Table 3 presents values of the enthalpy increment above 298 K fit to the equation

$$(H^\circ_T - H^\circ_{298})/R = a + bT + cT^2 + dT^3. \quad (2)$$

Values of $\Delta_f H^\circ_{298}/R$, S°_{298}/R, and $(H^\circ_{298} - H^\circ_0)/R$ are presented in Table 4.

The quantity S°_T/R for a substance may be found from the relationship

$$S^\circ_T/R = -(G^\circ_T - H^\circ_{298})/RT + (H^\circ_T - H^\circ_{298})/RT. \quad (3)$$

The equations given for $-(G^\circ_T - H^\circ_{298})/RT$ and $(H^\circ_T - H^\circ_{298})/R$ represent the tabulated values within typical limits of ± 0.01 or ± 0.01 kK over their applicable temperature ranges. The equations were derived by fitting tabular data for the particular functions cited; they are not direct integrations of heat capacity equations. Because of the nature of the polynomial fits, values derived by differentiating these equations do not accurately represent thermodynamic properties, e.g., heat capacities.

2.3. Condensed Phase Thermochemical Data

This section gives background information on alkali oxide condensed phases and additional information on the selected thermodynamic data presented in Tables 1–4 and referenced in Table 5.

a. Li–O Phases

The Li–O phases important above room temperature are Li_2O and Li_2O_2.[34] Lithium superoxide LiO_2 and ozonide LiO_3 are reported to be unstable, even at relatively high oxygen pressures and low temperatures.[34–38]

Li(s,l)—thermodynamic functions for the liquid above 1300 K were calculated for an estimated heat capacity $C^\circ_p/R = 3.45$. The enthalpy of fusion of Malaspina *et al.*[39] is in good agreement with the selected value.

Li_2O(s,l)—values of the enthalpy and Gibbs energy function above 1125 K were calculated by integrating estimated heat capacities including the effect of a diffuse disordering transition[40] in the antifluorite-type crystal lattice.[1] The recent heat capacity measurements of Tanifuji and Nasu[41] agree with the selected values within experimental error. JANAF[17] selected 1843 K as the melting point of Li_2O on the basis of the work of Van Arkel *et al.*[42] The value shown in Table 1 was taken from the work of Brewer and Margrave[43] and the subsequent determinations by Papin *et al.*,[44] Akiyama *et al.*,[45] and Ortman and Larsen.[46]

Li_2O_2(s,l)—the melting temperature, enthalpy of fusion, and liquid heat capacity were estimated.

b. Na–O Phases

The Na–O phases important above room temperature are Na_2O, Na_2O_2, and NaO_2.[34,35] The data on the thermodynamics of liquid sodium oxide solutions by Leffler and Wiederhorn[47] were not reviewed in the present study. The selected thermodynamic properties of the individual substances were taken from the sources cited below.

Na(s,l)—the heat capacities of Hultgren *et al.*[48] were accepted below 1100 K; above this temperature they were smoothly merged with the values of Fredrickson and Chasanov,[49] which extended to 1500 K. Above this temperature, the heat capacity of Na(l) was estimated to be $C^\circ_p/R = 3.80$. The heat capacities were integrated to give values of the Gibbs energy function and enthalpy increments above 298.15 K.

NaO_2(s,l)—the thermodynamic properties of the liquid were calculated using estimated values of the enthalpy of fusion and liquid heat capacity.

Na_2O(s,l)—values of the Gibbs energy function and enthalpy increments between 298.15 and 1300 K were calculated by integrating the heat capacities of Fredrickson and Chasanov.[50] Na_2O(s) is expected to undergo a diffuse disordering transition of its antifluorite crystal lattice[1,40] above the temperatures of the heat capacity measurements of Fredrickson and Chasanov and of Grimley and Margrave.[51] Estimated heat capacity values that included contributions of the disordering transition estimated by analogy with K_2S(s) were used to calculate values of the Gibbs energy function and enthalpy increments above 1300 K. Neither Fredrickson and Chasanov[50] nor Henry *et al.*[52] observed the solid-phase transitions reported by Bouaziz *et al.*[53] at 1023.2 and 1243.2 K, which were not included in the present work. The selected enthalpy of formation was derived from the measurements of O'Hare[54] and Gross and Wilson.[55]

Na_2O_2(s,l)—estimated values of the enthalpy of fusion and liquid heat capacity were used to derive Gibbs energy function and enthalpy increment values for the liquid.

c. K–O Phases

The solid phases of the K–O system were reviewed by Elliott[34] and Shunk,[56] and more recently by Byker *et al.*[57] The phases reported are K_2O, K_2O_2, KO_2, and KO_3. KO_3 reportedly decomposes at 333 ± 2 K[56]; thus, it is not a factor in high temperature vaporization processes. Data on the potassium oxides is limited and of uncertain quality. Different observers have reported significantly different vaporization behavior for solid K_2O and K_2O_2; in particular, Leffler and Wiederhorn[47] and Petrocelli[58] observed greater O_2 dissociation pressures over K_2O_2 than those calculated from thermodynamic data. The selected enthalpies of formation shown in Table 4 are in good agreement with the NBS[16] and JANAF[17] values and are reasonably consistent with trends in the other alkali oxides. Nevertheless, new studies are needed.

K(s,l)—thermodynamic functions were calculated using the estimated heat capacity values $C_p/R = 2.92 + 7.24 \times 10^{-4}T$ above 1300 K.

KO_2(s,l)—the melting temperature is uncertain because of large impurity effects; experimental values of T_{fus} range

from 653 to 782 K. Byker *et al.*[57] estimated $T_{fus} = 865$ K and $\Delta_{fus}H/R = 1.624$ kK from an analysis of phase diagram data. The heat capacity of the liquid was estimated as $C_p/R = 12.6$ for calculation of Gibbs energy function and enthalpy increment values.

K_2O(s,l)—no experimental heat capacity or entropy data were found. The entropy at 298.15 K was estimated by the Latimer relation $S°(298\ K)/R = 1.5 \ln M + 3B$, where M is the species gram formula weight and B a constant whose value was interpolated for K_2O(s) on a plot of ln M vs B for solid alkali metal M_2O oxides. The resulting value, $S°(298\ K)/R = 11.34$, is in good agreement with the estimated value given in JANAF.[17] Both JANAF and Eliezer *et al.*[59] estimated heat capacities for solid K_2O. The JANAF values are too large, and the values of Eliezer *et al.* are for temperatures over 1000 K. The melting temperature is uncertain; the experimental value of 919 + 5 K of Natola and Touzain[60] based on DTA of a 30 mg specimen was rejected because the likely interactions with the Pyrex container and the noncongruent vaporization of K_2O would both lower the observed melting temperature. Simmons *et al.*[61] reported a melting temperature of 1370 K based on analogy to the melting temperature of KCl, NaCl, and Na_2O. The thermodynamic functions for condensed K_2O of the present work were calculated using heat capacities estimated by analogy with the other alkali M_2O oxides, including the effects of a diffuse disordering transition in the antifluorite crystal lattice.[1,40] The melting temperature given in the present work was estimated by analogy to K_2S and Na_2S (Ref. 17, March 31, 1978 supplement) and Na_2O. The enthalpy of formation and K_2O(s) reported by JANAF[17] and others was taken from the solution calorimetric work of Rengade[62]; a modern determination is needed.

K_2O_2(s,l)—heat capacity values given in JANAF[17] were used, along with the value of $S°(298\ K)/R$ estimated using Latimer's rule, to calculate Gibbs energy function and enthalpy increment values for the solid. The calculated values of the Gibbs energy function were used along with the pressure data of Riley[63] and Kazarnovskii and Raikhshtein[64] for the reaction

$$2KO_2(s) = K_2O_2(s) + O_2(g)$$

to derive the enthalpy of formation. Byker[57] had done this calculation with the JANAF Gibbs energy values. The JANAF value of the enthalpy of formation, derived from earlier sources, is in good agreement with the selected value.

d. Rb–O Phases

The Rb–O phases important above room temperature are Rb_2O, Rb_2O_2, and RbO_2.[34,35,56] The ozonide RbO_3 has been reported,[34] as well as the suboxide phases Rb_6O and Rb_9O_2[65]; these phases are not stable at high temperatures. Thermodynamic data for individual substances was taken from the sources given below.

Rb(s,l)—thermodynamic values above 1300 K were calculated from estimated heat capacities.

RbO_2(s,l)—Paukov *et al.*[66] measured the heat capacity of RbO_2(s) from 13 to 298 K. Their values of heat capacity, entropy, and $(H°_{298} - H°_0)/R$ were adopted. The melting temperature was taken from Centnerszver and Blumenthal.[67] Gibbs energy function and enthalpy increment values were calculated using estimated values of the heat capacity above 298.15 K and an estimated enthalpy of fusion.

Rb_2O(s,l)—no experimental heat capacity or entropy data were found. The entropy at 298.15 K was estimated by the method used for K_2O. Heat capacity values for the solid were estimated by analogy to the other alkali metal M_2O oxides and included the effects of a diffuse disordering transition in the antifluorite crystal lattice.[1,40] The melting temperature was estimated from a plot of T_{fus} vs ln M, where M is the gram formula weight, for the alkali metal M_2O oxides. The heat capacity and enthalpy of transition data were used to calculate Gibbs energy function and enthalpy increment values.

Rb_2O_2(s,l)—the heat capacity above 298.15 K was estimated by analogy to that of Rb_2O and the difference between $C°_p$ values for Na_2O_2 and Na_2O. The entropy at 298.15 K was estimated as for K_2O_2. The liquid heat capacity was estimated. The estimated entropy and heat capacities were used to calculate Gibbs energy function and enthalpy increment values. The enthalpy of formation was calculated using the pressure measurements of Kraus and Petrocelli[68] for the reaction

$$2RbO_2(s) = Rb_2O_2(s) + O_2(g).$$

This enthalpy of formation was calculated by both second- and third-law methods; the second-law method gave a value of $\Delta_fH°_{298}/R$ 1.6 kK less negative than the selected value. Earlier values of the enthalpy of formation included a value estimated by de Forcrand[69] and a value derived from the doubtful pressure measurements of Centnerszver and Blumenthal.[67] The selected value is 0.5 kK more negative than the NBS[16] value and 2.9 kK more negative than the IVTAN[26] value.

e. Cs–O Phases

Knights and Phillips[70] reviewed the literature on condensed phases of the Cs–O system and reported the solid phases Cs_2O, Cs_2O_2, CsO_2, Cs_7O, Cs_4O, Cs_7O_2, Cs_3O, and CsO_3. Simon[65] reported the phase $Cs_{11}O_3$ rather than Cs_7O_2. Except for Cs_2O, Cs_2O_2, CsO_2, and Cs_3O, which decomposes peritectically at 437 K, the solid phases undergo decomposition at relatively low temperatures.[70] Knights and Phillips reported thermodynamic data, which were not evaluated in the present work, for liquid cesium oxide solutions. Sources of data selected for individual substances are given below.

Cs(s,l)—Behrens *et al.*[71] found that the Gibbs energy functions derived from the heat capacities of Hultgren *et al.*[48] are inconsistent with Cs vaporization data. On this basis, the JANAF[17] values of the thermodynamic functions for condensed Cs were adopted. The data were estimated above 1300 K.

CsO_2(s,l)—The entropy at 298 K was estimated using Latimer's rule. Values of the Gibbs energy function and enthalpy increments were calculated from heat capacities estimated by adding the heat capacity of Cs_2O to the heat capacity difference between NaO_2 and Na_2O.

Cs_2O(s,l)—Flotow and Osborne[72] measured the heat capacity of Cs_2O from 5 to 350 K, and extrapolated their results to the melting temperature. Their data for the Gibbs energy function, $(H^\circ_{298} - H^\circ_0)/R$, and $(H^\circ_T - H^\circ_{298})$ were accepted. Cs_2O crystallizes in a $CdCl_2$-type rhombohedral structure,[1] and thus does not undergo the high temperature antifluorite disordering transition expected for the other dialkali monoxides. Thermodynamic functions of the liquid were calculated from estimated heat capacities.

Cs_2O_2(s,l)—the entropy at 298.15 K was estimated by Latimer's rule. Values of the Gibbs energy function and enthalpy increments were calculated from heat capacities estimated by analogy to Cs_2O and the difference between Na_2O and Na_2O_2. The enthalpy of formation was calculated from the dissociation pressure measurements of Berardinelli and Kraus[73] for the reaction

$$2CsO_2(s) = Cs_2O_2(s) + O_2(g).$$

Berardinelli and Kraus[73] began their measurements with specimen compositions near CsO_2 and monitored composition change by mass loss, which was assumed to be due to O_2 only. This assumption, valid for the decomposition of CsO_2 to Cs_2O_2, is demonstrably wrong for vaporization of Cs_2O_2; thus, the pressure data reported for the reaction

$$Cs_2O_2(s) = Cs_2O(s) + 1/2O_2(g)$$

probably do not correspond to this equilibrium. IVTAN[26] reported the value $\Delta_f H^\circ_{298}/R = -54 \pm 3$ kK, probably based on the estimation of de Forcrand.[69]

2.4. Vapor Species Thermochemical Data

a. Discussion

This section gives background information on alkali oxide gas species and additional information on the selected thermodynamic data presented in Tables 1–4 and referenced in Table 5. The alkali metal–oxygen vapor species reviewed below are grouped by generic molecular formula rather than by their alkali metal constituent because of the generally related molecular properties of the homologous species.

b. M(g) Species

M(g) species—Hultgren's enthalpies of formation,[48] which incorporated data not reviewed by JANAF[17] were used.

c. MO(g) Species

The spectroscopic constants of the gaseous alkali monoxides are based almost entirely on *ab initio* calculations, as summarized for the most part by Huber and Herzberg.[74] Additionally, the vibrational frequency of RbO and the internuclear distance in CsO were estimated by analogy with trends in the diatomic alkali fluorides, chlorides, and oxides, while the energy of the first excited electronic state of CsO was estimated by extrapolating the values for the lighter alkalis. The selected constants used in calculating thermodynamic functions are summarized in Table 6.

Because of the scarcity of thermochemical data for all of the gaseous monoxides but LiO, the dissociation energies of the MO species were calculated by means of the Rittner polarizable ion model[29,30] as an aid in evaluating the experimental results and fixing trends in the series. Input parameters for the Rittner calculations are given in Table 7, while the calculated and experimental dissociation energies are compared in Table 8. In view of the reasonably good agreement between the two values for LiO, NaO, and KO, the Rittner calculated values for RbO and CsO were selected for evaluating the standard enthalpies of formation.

Table 6. Molecular constants of the alkali metal MO vapor species.[a]

	$r_e \times 10^8$ (cm)	ω (cm^{-1})	Electronic ground state degeneracy	Electronic excited state degeneracy	T_e (cm^{-1})
LiO	1.695	852	2	2	2330
NaO	2.05	500[b]	2	2	1500
KO	2.22	384	2	2	347
RbO	2.28	340[c]	2	2	606
CsO	2.39[c]	314[d]	2	2	1000[c]

[a] Unless otherwise indicated, values were taken from reference 74.

[b] From the calculations of O'Hare and Wahl[112].

[c] Estimated by the method given in the text.

[d] From matrix isolation studies of Spiker and Andrews[113].

d. MO_2(g) Species

The gaseous alkali dioxide species LiO_2, NaO_2, KO_2, RbO_2, and CsO_2 have all been identified by low temperature matrix isolation spectroscopy, but these species have not been directly observed by mass spectrometry in any of the investigations reported to date. However, it seemed prudent

Table 7. Values of atomic and molecular constants used in Rittner electrostatic model calculations of the dissociation energies of alkali metal MO vapor species.[a]

	r x 10^8 [b] (cm)	$\alpha(M^+) \times 10^{24}$ [c] (cm^3)	k x 10^{-5} [d] (dyne/cm)	IP[e] (eV)
LiO	1.695	0.03	2.08	5.392
NaO	2.05	0.20	1.54	5.139
KO	2.217	1.00	1.00	4.341
RbO	2.278	1.70	1.00	4.197
CsO	2.39	2.50	0.90	3.894

[a] r--internuclear distance; α--dipole polarizability; k--force constant; IP--ionization potential; the electron affinity of O was 1.465 eV[17]; the polarizability of O^- was 1.0 x 10^{-24} cm^3.[105]

[b] References in table 5.

[c] Reference 114.

[d] Calculated from constants given in table 6.

[e] Reference 115.

Table 8. Enthalpies of formation and dissociation energies of alkali metal MO vapor species.

	$\Delta_f H^\circ_{298}/R$ (kK)	D°_0/R (kK)	Method	Reference
LiO	9.1 ±1.0	39.6 ±1.0	Experimental	94
	8.3 ±0.8	40.4 ±0.8	Experimental	105
	8.6 ±2.5	40.1 ±2.5	Experimental	80
	8.7 ±0.5	40.0 ±0.5	Rittner model	This work
	8.3 ±0.8	40.4 ±0.5	(Selected value)	
NaO	12.6 ±0.3	29.8 ±0.3	Experimental	76
	13.3 ±0.5	29.1 ±0.5	Rittner model	This work
	12.6 ±0.3	29.8 ±0.3	(Selected value)	
KO	7.4 ±2.5	33.0 ±2.5	Experimental	107
	7.2 ±0.5	33.2 ±0.5	Rittner model	This work
	7.2 ±0.5	33.2 ±0.5	(Selected Value)	
RbO	7.1 ±0.5	32.8 ±0.5	Rittner model	This work
			(Selected Value)	
CsO	4.9 ±0.5	33.9 ±0.5	Rittner model	This work
			(Selected Value)	

to include data for these species, since they may be important under oxidizing conditions. The molecular constants used to calculate thermodynamic functions for the alkali MO_2 vapor species are shown in Table 9.

The only experimental enthalpy data found for these species are those for NaO_2 deduced from the flame studies of McEwan and Phillips[75] who reported data for the reaction

$$NaO_2(g) = Na(g) + O_2(g).$$

However, these data predict $NaO_2(g)$ to be a major species over $Na_2O(s)$ under neutral Knudsen cell conditions, contrary to observations.[76] We believe that the flame data on $NaO_2(g)$, which are indirect, are in error.

Since none of the MO_2 vapor species has been observed under neutral Knudsen cell conditions, lower limits for the enthalpies of formation were estimated by considering the reaction

$$2MO_2(g) = M_2O(g) + 3/2O_2(g),$$

for which the Gibbs energy change is given by the equation

$$\Delta G/RT = \Delta\left[-(G^\circ_T - H^\circ_{298})/RT + \Delta_f H^\circ_{298}/R\right] = \ln[p(M_2O)p(O_2)^{3/2}/p(MO_2)^2], \quad (4)$$

and taking 10^{-10} bar as the limit of detection in the mass spectrometric experiments. Third-law calculations combined with the established M_2O data yield the lower limit values for the MO_2 enthalpies of formation. The values are uncertain, since detection limits in the mass spectrometric investigations are somewhat variable.

Table 9. Molecular constants of the alkali metal MO_2 vapor species.[a]

	r(M-O)x10^8 (cm)	<O-M-O (deg)	ω_1 (cm^{-1})	ω_2 (cm^{-1})	ω_3 (cm^{-1})
LiO_2[b,c,d]	1.77	44	1097	699	492
NaO_2[c,e,f]	2.07	37.5	1080	391	333
KO_2[c,g]	2.28	32.6	1108	308	300
RbO_2[c,g,h]	2.57	28.8	1110	255	283
CsO_2[c,g,h]	2.67	27.7	1114	237	269

[a] The molecules have C_{2v} geometry, a symmetry number of 2, and were assumed to have an electronic ground state degeneracy of 2.
[b] Reference 86.
[c] Reference 89.
[d] Reference 116.
[e] Reference 87.
[f] Reference 117.
[g] Reference 88.
[h] Reference 118.

e. $M_2(g)$ Species

$M_2(g)$ species—the low dissociation energies of the diatomic alkali metal species require that the statistical methods used to evaluate thermodynamic functions from molecular data utilize accurate rotation–vibration energy levels and correct cutoff procedures for dissociating states. Several groups have performed these calculations for Li_2, Na_2, and K_2; the calculations of Feber and Herrick[77] were used in the present work. In the absence of more accurate calculations, data for $Cs_2(g)$ were taken from JANAF.[17] Spectroscopic data from Hultgren *et al.*[48] were used to calculate the Gibbs energy functions for Rb_2 given in the present work. Only the nondissociating ground state and one excited state were used in these calculations. Since the diatomic elemental species are minor components of the vapor, these approximations should not introduce significant error into the vapor pressure calculations. The enthalpy of formation of Li_2 was derived from the accurate *ab initio* dissociation energy of Konowalow and Olson.[78] The enthalpies of formation of the remaining M_2 species were calculated from the dissociation energies compiled by Huber and Herzberg.[74] The data of Piacente *et al.*[79] were also considered for Rb_2.

f. $M_2O(g)$ Species

On the whole, the gaseous dialkali monoxide species have been studied in considerably more detail than the other alkali oxide species. Nevertheless, there are considerable uncertainties in some of the results, and the molecular constants needed for calculation of thermodynamic functions are incomplete. The equilibrium data for the Li and Na species appear to be reliable; those for the K, Rb, and Cs species are less certain, and further experimental investigations are needed.

Table 10 lists the selected molecular constants used in calculating thermodynamic functions. Experimentally un-

Table 10. Molecular constants of the alkali metal M_2O vapor species.[a]

	r(M-O)x10^8 (cm)	<M-O-M (deg)	ω_1 (cm^{-1})	ω_2 (cm^{-1})	ω_3 (cm^{-1})
Li_2O	1.60[b]	180[c]	(760)[c]	(140)[c,d]	987[c]
Na_2O	(1.95)	(180)	(450)	(100)[d]	(600)
K_2O	(2.12)	160[e]	(301)	(80)	500[e]
Rb_2O	(2.17)	160[e]	(284)	(70)	473[e]
Cs_2O	(2.28)	140[e]	(305)	(60)	455[e]

[a] r--internuclear distance; <--angle; ω_1, ω_2, ω_3 --wave numbers of fundamental vibrations. The symmetry number was assumed to be 2. The electronic ground state was assumed to be nondegenerate, and no excited electronic states were included in the calculations. Values in parentheses are estimated, and those not referenced are from the present study.

[b] Reference 119.

[c] Reference 17.

[d] Doubly degenerate vibrational mode.

[e] Reference 113.

Table 11. Molecular constants for the alkali metal M_2O_2 vapor species.[a]

	r(O-O)x10^8 (cm)	r(M-M)x10^8 (cm)	<O-M-O (deg)	$I_xI_yI_z$x10^{117} (g^{3}cm^6)
Li_2O_2	1.50[b]	2.91[c]	54	1.16x10^2
Na_2O_2	1.50	3.67	44	2.21x10^3
K_2O_2	1.50	4.02	41	8.70x10^3
Rb_2O_2	1.50	4.15	40	4.56x10^4
Cs_2O_2	1.50	4.37	38	1.35x10^5

[a] Unless otherwise indicated, values were estimated as described in the text. The symmetry was assumed to be D_{2h}, with a symmetry number of 4. The electronic ground state was assumed to be nondegenerate, and no excited electronic states were included in the calculations of thermodynamic functions.

[b] Reference 90.

[c] Reference 86.

known M–O distances were estimated using the ratio of Li–O distances in LiO and Li_2O and the known or estimated M–O distance in the monoxides. Except for Na_2O, the unsymmetrical stretching frequency has been observed by matrix infrared spectroscopy. For Na_2O, this frequency was estimated by interpolation. For the Li and Na species, estimated values of the other vibrational frequencies were taken from White *et al.*[80] and from Hildenbrand and Murad.[76] Values for the K, Rb, and Cs species were estimated by analogy to the values for the Li and Na species.

The selected enthalpies of formation of the M_2O species shown in Table 4 are all based on equilibrium measurements. For $Li_2O(g)$, the value was taken from the concordant results of Hildenbrand *et al.*,[81] White *et al.*,[80] Norman and Winchell,[82] and Ikeda *et al.*[83] The value for Na_2O was taken from Hildenbrand and Murad[73] and Norman and Winchell.[82] The results of Gorokhov *et al.*[84,85] and of Norman and Winchell were used to derive the selected enthalpies of formation for $Rb_2O(g)$ and $Cs_2O(g)$.

g. $M_2O_2(g)$ Species

Data for the alkali metal M_2O_2 vapor species are less complete and less certain than for the corresponding M_2O or MO species. All have been observed by low temperature matrix isolation spectroscopy, but the fundamental vibrational frequencies have been only partially assigned, and information about molecular geometries is incomplete. Mass spectrometric studies of reaction equilibria involving Li_2O_2, K_2O_2, and Cs_2O_2 have been made, but no data is available for Na_2O_2 or Rb_2O_2.

The selected molecular constants are shown in Table 11. In accordance with the matrix spectra of Andrews and co-workers,[86–89] the M_2O_2 species were regarded as planar D_{2h} molecules with symmetry numbers of 4. The O–O distances in the molecules were taken as 1.5×10^{-8} cm, in accord with data on the solid alkali peroxides[35] and the *ab initio* results of Yates and Pitzer[90] on Li_2O_2. The M–O distances were estimated by multiplying the value of r(M–O) of the MO(g) species by the ratio $r(M–O,Li_2O_2,g)/r(M–O,LiO,g) = 1.64/1.695$.[90,91]

The selected vibrational frequencies of the M_2O_2 molecules are given in Table 12. Unobserved vibrational frequencies were estimated by multiplying the frequencies of Li_2O_2[86,90] by the ratio of comparable frequencies in the species M_2O to those in Li_2O. For this correlation, the A_g, A'_g, and B_{1g} M_2O_2 modes were assumed to scale as the M_2O ω_1 mode; the B_{1u} mode of M_2O_2 as the ω_2 mode of M_2O; and the B_{3u} mode of M_2O_2 as the ω_3 mode of M_2O. Experimental values are available for the B_{2u} modes for each of the M_2O_2 species, so that predicted and observed values can be compared; except for Na_2O_2, where the predicted frequency is high by 43 cm^{-1}, the agreement is within 21 cm^{-1}.

Enthalpies of formation derived from mass spectrometric data were selected from the concordant experimental values for Li_2O_2,[80,92–94] K_2O_2,[85] and Cs_2O_2.[82,85] For Na_2O_2 and Rb_2O_2, enthalpies of formation were estimated by interpolating the energy of the reaction.

$$M_2O_2(g) = 2MO(g),$$

via a plot $[D_0(M_2O_2 - 2D_0(MO)]$ vs $D_0(MO)$ for the alkali metals.

Table 12. Vibrational fundamentals of alkali metal M_2O_2 vapor species. (Units: cm^{-1})

	Vibrational Mode					
	B_{1u}	B_{2u}	B_{3u}	A_g	A'_g	B_{1g}
Li_2O_2	94[a]	796[b]	446[b]	954[a]	741[a]	639[a]
Na_2O_2	70[c]	525[d]	254[d]	565[c]	440[c]	380[c]
K_2O_2	55[c]	433[e]	226[c]	380[c]	290[c]	250[c]
Rb_2O_2	47[c]	389[e]	214[c]	356[c]	280[c]	240[c]
Cs_2O_2	40[c]	357[f]	206[c]	380[c]	300[c]	260[c]

[a] Reference 90, ab initio calculations.

[b] Reference 86, experimental.

[c] This work, estimated.

[d] Reference 87, experimental.

[e] Reference 88, experimental.

[f] Reference 89, experimental.

h. Other Species

The species Li_3 was reported in a mass spectrometric study of the vaporization of pure lithium.[95] Kimoto *et al.*[96] did not observe Li_3 in a similar experiment. The theoretical results of Gerber and Schumacher[97] and of Kendrick and Hillier[98] were used to estimate the molecular constants: C_{2v} geometry, $\sigma = 2$, electronic ground state degeneracy $= 2$, $r_e(\text{Li–Li}) = 2.9$ Å, $\angle\text{Li–Li–Li} = 100°$, $\omega_1 = 230\ cm^{-1}$, $\omega_2 = 115\ cm^{-1}$, $\omega_3 = 210\ cm^{-1}$. The enthalpy of formation was calculated from the vaporization data of Wu.[95] The calculations of Sec. 3 indicate that Li_3 is a minor species in the high temperature vaporization of lithium oxides.

The species Li_3O has been reported in mass spectrometric investigations of the vaporization of Li_2O by Wu *et al.*,[92] Ikeda *et al.*,[83] and Kimura *et al.*[94] The pressures reported for this species were near instrumental sensitivity limits and differ significantly among the different investigators. Approximate thermodynamic functions for $Li_3O(g)$ were estimated from the molecular constants for $Li_2O_2(g)$ and rhombic Li_4 clusters[99,100] and were used in third-law calculations to estimate the enthalpy of formation from the vaporization data of Wu *et al.* and of Kimura *et al.*

3. High Temperature Equilibria and Vaporization Rates

3.1. Equilibrium Properties of Alkali Oxides

The solid phases relevant to high temperature vaporizaiton processes are the M_2O dialkali monoxide, the M_2O_2 peroxide, and the MO_2 superoxide. Phases of the composition M_2O_3 have been reported for alkali metals except lithium,[35] but their existence as pure equilibrium phases has not been substantiated.[1,56,57,70] Several general trends exist in the properties of alkali oxides. The higher oxide condensed phases become more stable relative to the dialkali monoxide as the size of the metal ion increases. This trend is illustrated by the synthetic methods used for oxide production.[35,57,72,101] Direct oxidation of the metal at moderate temperatures in dry air produces Li_2O, Na_2O_2, KO_2, RbO_2, and CsO_2. NaO_2 is produced by high temperature reaction of Na_2O_2 with high pressure oxygen. Thermal decomposition of the corresponding superoxides yields K_2O_2, Rb_2O_2, and Cs_2O_2, and decomposition of Na_2O_2 gives Na_2O. The dialkali monoxides of K, Rb, and Cs are produced by reacting the peroxides with excess metal, then removing the remaining metal by distillation.

For lithium, the only important high temperature solid oxide is the dialkali monoxide. For sodium, the dialkali monoxide is stable under neutral or reducing conditions above about 400 K, but in dry air the peroxide is stable up to its melting point. Either the peroxide or superoxide of K, Rb, or Cs is stable under neutral or oxidizing conditions at high temperatures. The existence of several possible oxide phases complicates the study and description of vaporization processes for K, Rb, and Cs oxides, especially when low-melting liquids are considered.

The information needed to characterize the vaporization behavior of oxides was discussed by Brewer in his 1953 review.[1] The most important facts to be established are the identities of the important vapor species and the effects of vaporization on condensed phase compositions. When these two factors are known, the vaporization equilibria can be described and quantitatively calculated if the necessary thermodynamic data are available. The important vapor species are reasonably well established for alkali metal–oxygen systems; unfortunately, changes in condensed phase composition during vaporization are only partially known.

According to the phase rule, the intensive variables of an alkali metal–oxygen system depend only on temperature if two condensed phases and one gas phase are present. If only one condensed phase and a gas phase are present, one additional variable must be specified to define the state of the system. This requirement can be met by specifying the oxygen potential or the elemental composition of the vapor phase. Congruent vaporization, in which the overall elemental composition of condensed and vapor phases are the same, is a particular example of a one-solid-phase vaporization process in which the state of the chemical system is specified by temperature and gas phase composition. Experimentally, solid Li_2O and Na_2O vaporize congruently under neutral conditions.[76,81,102] Thermodynamic data indicate that solid K_2O_2, Rb_2O_2, and Cs_2O_2 also vaporize congruently.

3.2. Mathematics of Vaporization Calculations

The calculations that follow are applicable to the vaporization of pure solid and liquid phases under conditions where condensed phase composition changes are negligible; vaporization from solution phases is beyond the scope of the present work, and the necessary data are for the most part unavailable. The properties considered are the vapor pressures of principal vapor species and the rate of mass loss per unit surface area, both as functions of temperature.

For many vaporization conditions one or two vapor species are predominant, and calculation of the chemical

equilibrium from thermodynamic data is straightforward. Calculations can be more complicated when several species are present in significant quantities. The following procedure is a general method for calculating the equilibrium pressures of vapor species in equilibrium with a condensed phase of known composition.

The chemical species present at equilibrium in the vaporization of a condensed binary oxide can be described mathematically as being formed by linear combination of the vaporizing oxide M_bO_c and oxygen O_2 according to the general reaction for the production of species i,

$$d(\mathrm{i})M_bO_c(\mathrm{s,l}) + e(\mathrm{i})O_2(\mathrm{g}) = M_x(\mathrm{i})O_y(\mathrm{i})(\mathrm{s,l,or\ g}),$$

where e(i) may be zero or a negative number. The possible species include the vaporizing phase M_bO_c(s or l), considered to be species 1, and O_2(g) as well as the species produced by their linear combination. From mass balance,

$$d(\mathrm{i}) = x(\mathrm{i})/b, \tag{5}$$

and

$$e(\mathrm{i}) = [by(\mathrm{i}) - cx(\mathrm{i})]/2b. \tag{6}$$

We define the Gibbs energy of species i at temperature T as

$$G^\circ_T(\mathrm{i})/RT = (G^\circ_T - H^\circ_{298})/RT - \Delta_f H^\circ_{298}(\mathrm{i})/RT. \tag{7}$$

The Gibbs energy change for the reaction producing gaseous species i from M_bO_c(s or l) and O_2(g), $\Delta_r G^\circ_T$(i), is given by

$$\Delta_r G^\circ_T(\mathrm{i})/RT = G^\circ_T(\mathrm{i})/RT - d(\mathrm{i})G^\circ_T[M_bO_c(\mathrm{s\ or\ l})]/RT - e(\mathrm{i})G^\circ_T[O_2(\mathrm{g})]/RT, \tag{8}$$

and the equilibrium constant for producing gas species i is

$$K(\mathrm{i}) = \exp[-\Delta_r G^\circ_T(\mathrm{i})/RT] = p(\mathrm{i})/\{a(1)^{d(\mathrm{i})}p[O_2(\mathrm{g})]^{e(\mathrm{i})}\}, \tag{9}$$

where the pressures p(i) are considered low enough that they equal fugacities, and $a(1)$ is the activity of M_bO_c. If M_bO_c is a pure condensed phase, its activity is unity, and

$$p(\mathrm{i}) = K(\mathrm{i})p(O_2)^{e(\mathrm{i})}, \tag{10}$$

for the gas species. If the oxygen pressure is known, the pressure of each species i can be calculated from this equation.

For congruent vaporization, the vapor composition is the same as the condensed phase, and

$$\sum[p(\mathrm{i})x(\mathrm{i})] \Big/ \sum[p(\mathrm{i})y(\mathrm{i})] = b/c. \tag{11}$$

This leads to the expression

$$\sum[K(\mathrm{i})p(O_2)^{e(\mathrm{i})}\{cx(\mathrm{i}) - by(\mathrm{i})\}] = 0, \tag{12}$$

where summation is over the gaseous species present. In practice, this equation is solved for $p(O_2)$ by graphical interpolation or by numerical methods. The value found for $p(O_2)$ is then used in Eq. (10) to find the other partial pressures.

For the above calculations to correspond to equilibrium vaporization, they must be used for vaporization of the condensed oxide phase or phases stable under the particular vaporization conditions. Where more than one oxide phase is a possibility, the stable phase or phases must be determined.

Table 13. Oxygen pressures of two-solid-phase regions.

Log $p(O_2$,bar) = K + Q log T + RT + S/T + W/T^2

	K	Q	10^3R	10^{-3}S	10^{-6}W	T Range
Li_2O-Li_2O_2	879.52	-311.10	117.36	-54.94	3.21	298-450
Na_2O-Na_2O_2	-114.32	41.37	-11.03	0.22	-0.94	298-948
K_2O-K_2O_2	288.04	-95.49	25.88	-34.13	1.53	298-763
K_2O_2-KO_2	25.25	-8.44	3.62	-4.06	-0.10	298-763
Rb_2O-Rb_2O_2	585.01	-194.92	50.91	-59.31	3.75	350-843
Rb_2O_2-RbO_2	176.06	-60.68	19.69	-14.65	0.65	298-685
Cs_2O-Cs_2O_2	-94.23	36.87	-12.67	-8.96	-0.54	350-768
Cs_2O_2-CsO_2	143.81	-49.06	15.08	-12.83	0.59	298-723

Two condensed oxide phases of fixed composition at a given temperature are related by the equilibrium

$$\mathrm{Oxide\ (1)} = \mathrm{Oxide\ (2)} + f O_2(\mathrm{g}).$$

Oxide (1) is assumed to have the greater oxygen activity. The equilibrium constant for this reaction is

$$K_{eq} = a(2)p(O_2)^f/a(1). \tag{13}$$

If both condensed phases are present at equilibrium, their activities are unity, and the pressure of O_2 is given by the equation

$$p_{eq}(O_2) = K_{eq}^{(1/f)}. \tag{14}$$

Oxide (1) is the stable phase for O_2 pressure greater than $p_{eq}(O_2)$, and oxide (2) is stable for O_2 pressures less than $p_{eq}(O_2)$ at the given temperature. The calculated oxygen pressures for two-solid-phase regions are given as functions of temperature in Table 13.

3.3. Vaporization Rate Calculations

Maximum vaporization rates were calculated using the Hertz–Knudsen equation of classical kinetic theory, which applies to free vaporization from an uncontaminated surface at low pressures. For gas species i evolving from the surface, the maximum vaporization rate $dn(\mathrm{i})/dt$ in mol cm^{-2} s^{-1} is given by the equation

$$dn(\mathrm{i})/dt = p(\mathrm{i})/[2\pi M(\mathrm{i})RT]^{1/2}, \tag{15}$$

where M(i) and p(i) are the gram molecular weight and equilibrium partial pressure of vapor species i, and R and T are the molar gas constant and absolute temperature. Since 1 bar is 10^6 dyne cm^{-2} and R is 8.3144×10^6 erg mol^{-1} deg^{-1}, for pressures in bar, this is equivalent to

$$dn(\mathrm{i})/dt = 43.8\{p(\mathrm{i})/[M(\mathrm{i})T]^{1/2}\}\ \mathrm{mol\ cm^{-2}\ s^{-1}}. \tag{16}$$

Calculation of maximum vaporization rates is more difficult for noncongruent than for congruent processes. In general, solid phase activities during the vaporization process are not known, and calculated maximum vaporization rates of oxides that deviate from their original stoichiometry should be considered indicative rather than exact.[103] In the present work, maximum vaporization rates have been calcu-

lated for noncongruent, as well as congruent, vaporization. Only initial vaporization rates, for which no condensed phase composition changes have taken place, are considered. Vaporization rates are expressed in terms of the mass of originally present oxide M_bO_c lost as measured by the volatilization of metal atoms. The total mass loss thus calculated is

$$dm/dt = 44.3[M(M_bO_c)/b]\sum\{p(i)x(i)/[M(i)T]^{1/2}\}, \quad (17)$$

where dm/dt is the mass loss rate in g cm^{-2} s^{-1}, M_bO_c is the formula of the condensed oxide, and x(i) and M (i) are the number of gram atoms of metal per mole and gram molecular weight of gas species i.

Although actual vaporization may be slower, the calculated maximum vaporization rate is valuable as a rough guide to vaporization kinetics. Recent references on maximum vaporization rate calculations include works by Turkdogan[104] and Beruto *et al.*[103]

3.4. Vaporization Behavior under Representative Conditions

The calculated partial pressures of major species in equilibrium with stable alkali metal oxides are shown in the figures of this section as plots of log P vs $1/T$ for vaporization under conditions representative of those likely to be encountered experimentally. For each alkali metal–oxygen system, equilibrium partial pressures were calculated for vaporization in 0.2 bar of O_2, representing oxidizing conditions, for vaporization at a fixed oxygen potential of 10^{-15} bar, representing reducing conditions, and for vaporization of solid under neutral conditions. The calculations do not cover certain situations of practical interest. One of these is the vaporization of alkali metal–oxygen liquid solution phases, for which adequate thermodynamic data do not exist. Another is vaporization under conditions of decreased condensed phase activity, as in solutions of alkali oxides in silicate melts, which is beyond the scope of this work.

Species representing less than about 10^{-6} of the total pressure were omitted from the graphs, as were the gaseous dioxides, for which only upper limits of partial pressures could be calculated. The limiting stabilities indicate that the dioxides may be major species under oxidizing conditions, and it is important that their properties be determined.

a. Li–O System

Lithium oxide Li_2O is the stable condensed oxide phase at temperatures above about 380 K for vaporization at O_2 pressures up to 0.2 bar. The partial pressures of the major species in equilibrium with condensed Li_2O are shown in Figs. 1–3 for representative vaporization conditions. Liquid Li_2O was assumed to vaporize congruently under neutral conditions. Calculated maximum mass loss rates are shown in Fig. 4.

b. Na–O System

The equilibrium oxygen pressure for equilibrium of Na_2O_2(s) with NaO_2 is greater than 100 bar above 298 K, and disodium monoxide Na_2O is stable above about 400 K for

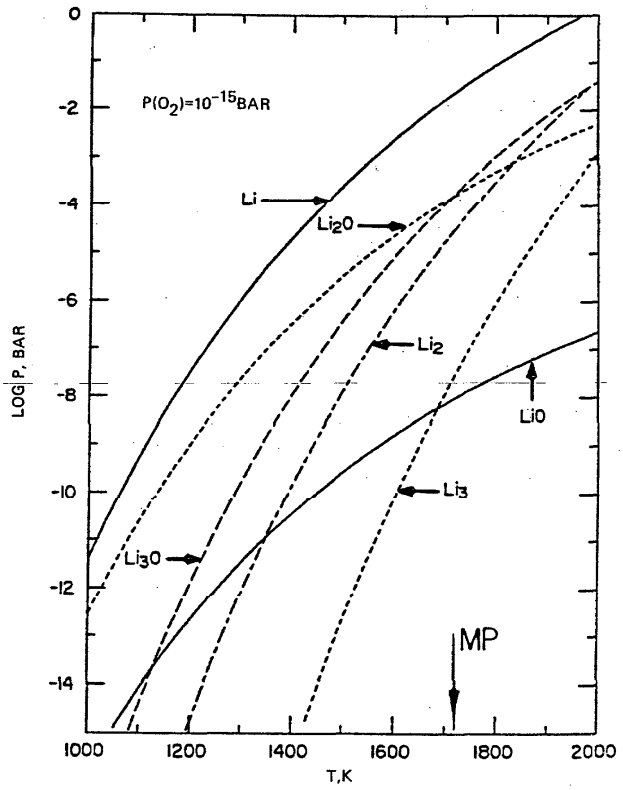

FIG. 1. Li_2O vaporization in 10^{-15} bar O_2.

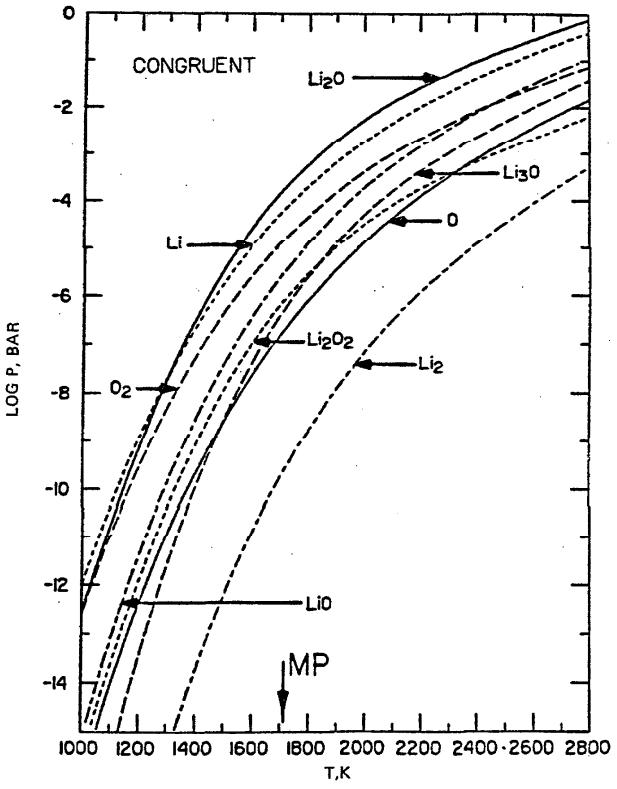

FIG. 2. Li_2O congruent vaporization.

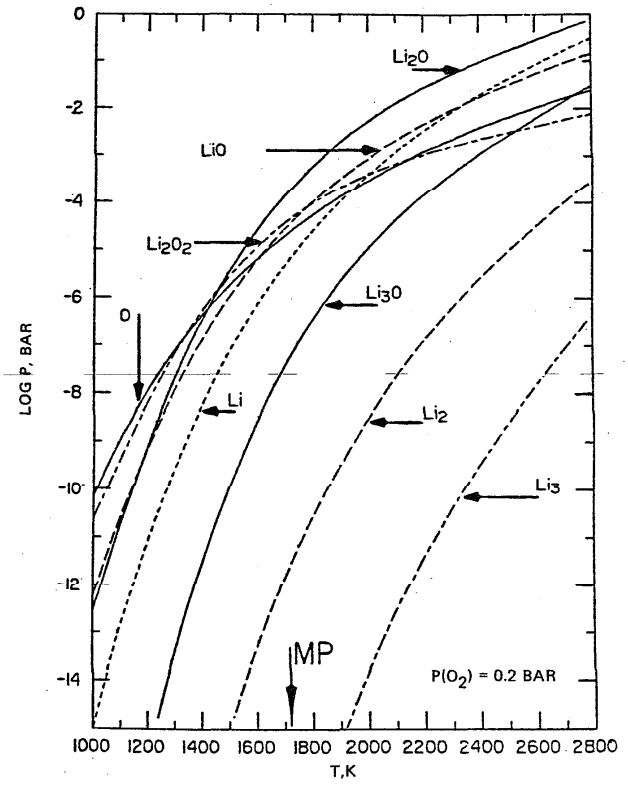

FIG. 3. Li_2O vaporization in 0.2 bar O_2.

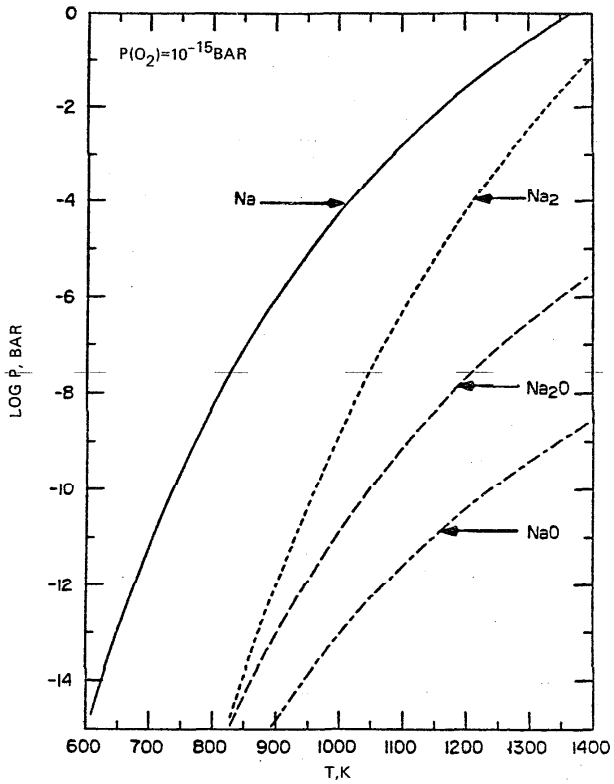

FIG. 5. Na_2O vaporization in 10^{-15} bar O_2.

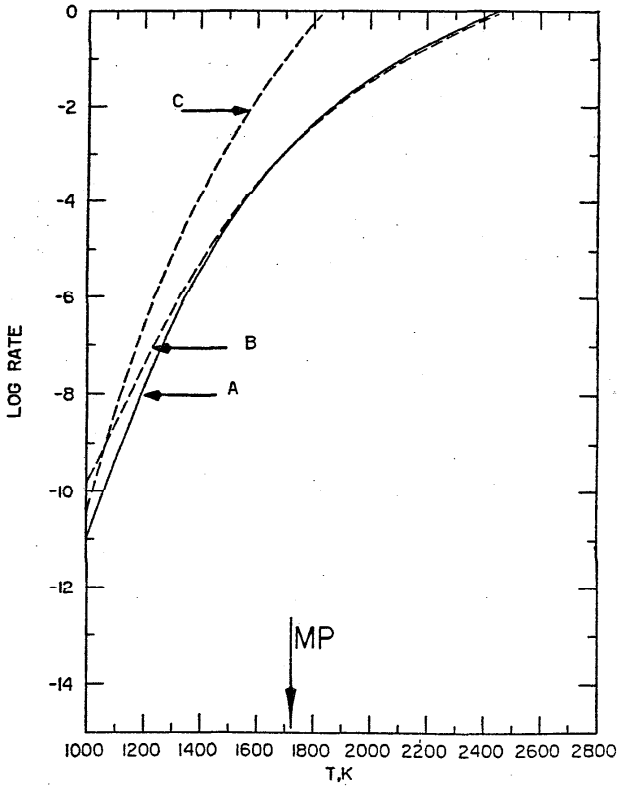

FIG. 4. Li_2O maximum vaporization rates. A—0.2 bar O_2; B—congruent vaporization; C—10^{-15} bar O_2. Rate units—g cm^{-2} s^{-1}.

congruent vaporization conditions. Liquid Na_2O was assumed to vaporize congruently under neutral conditions. The partial pressures of the major species in equilibrium with condensed Na_2O are shown in Figs. 5 and 6 for vaporization at an O_2 pressure of 10^{-15} bar and for congruent vaporization, respectively. The partial pressure curves in Fig. 7 are for vaporization of Na_2O_2 solid and liquid below 1150 K, and for vaporization of condensed Na_2O above this temperature, in 0.2 bar of O_2. Calculated mass loss rates for these vaporization conditions are shown in Fig. 8.

c. K–O System

Very little data are available on the vaporization of condensed potassium, rubidium, and cesium oxides, and the corresponding thermodynamic properties and composition changes during vaporization are known with less certainty than for lithium and sodium oxides. New studies of condensed phase vaporization equilibria and gas species thermodynamic properties are needed.

Partial pressures of species in equilibrium with K_2O at an O_2 pressure of 10^{-15} bar, for which K_2O is the stable solid phase above about 600 K, are shown in Fig. 9. Calculated partial pressures of the major species in equilibrium with condensed K_2O_2 are shown in Fig. 10 for congruent vaporization below the melting temperature; thermodynamic data indicate that K_2O_2 is the stable solid phase under these conditions. Byker *et al.*[57] concluded from the available evidence that under neutral conditions solid K_2O vaporizes to potassium-rich vapor with a resulting shift in overall condensed phase composition toward K_2O_2, and that the congruently

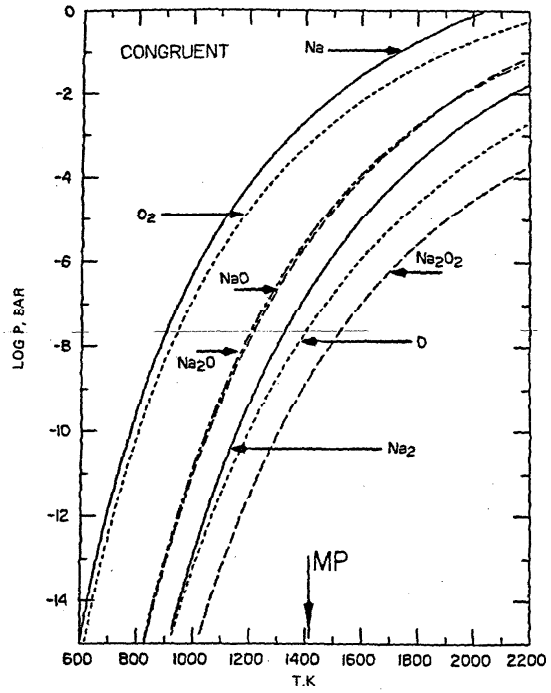

FIG. 6. Na_2O congruent vaporization.

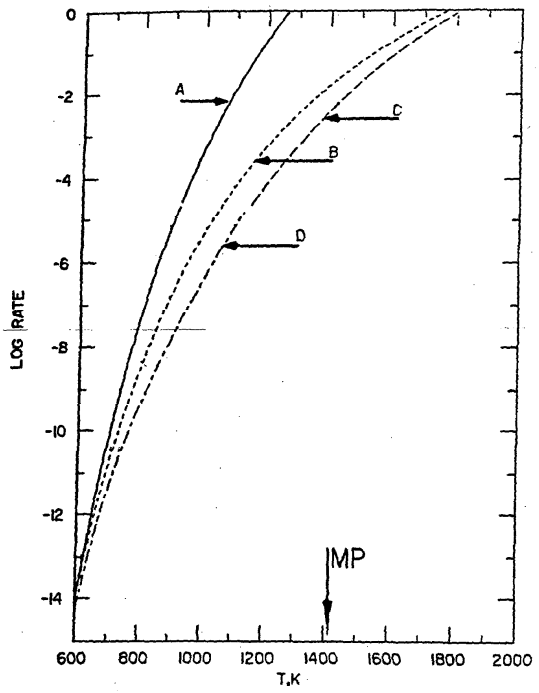

FIG. 8. Sodium oxide maximum vaporization rates. A—Na_2O in 10^{-15} bar O_2; B—Na_2O congruent vaporization; C—Na_2O in 0.2 bar O_2 above 1150 K; D—Na_2O_2 in 0.2 bar O_2 below 1150 K. Rate units—g cm^{-2} s^{-1}.

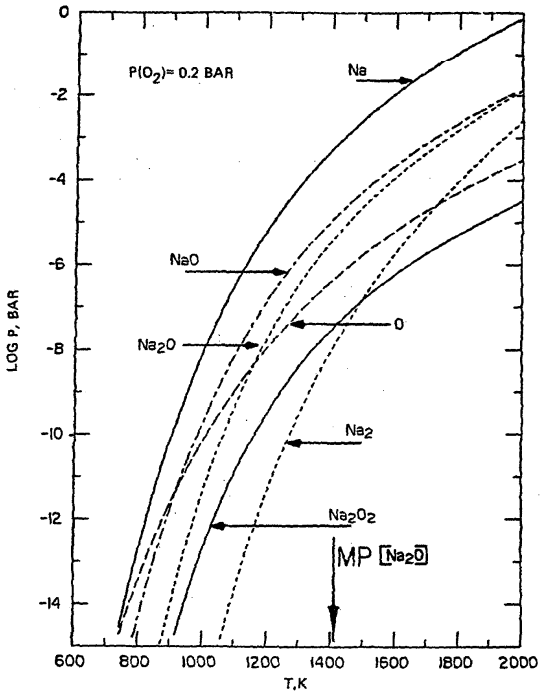

FIG. 7. Vaporization of sodium oxides in 0.2 bar O_2. The condensed phase is Na_2O_2 below and Na_2O above 1150 K.

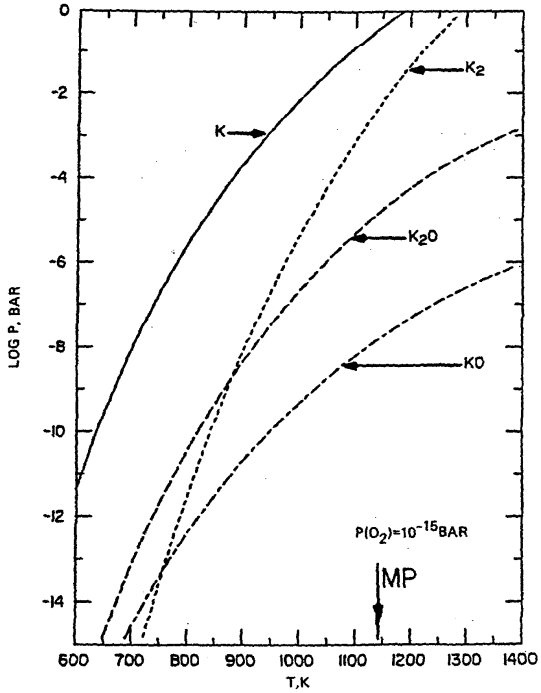

FIG. 9. K_2O vaporization in 10^{-15} bar O_2.

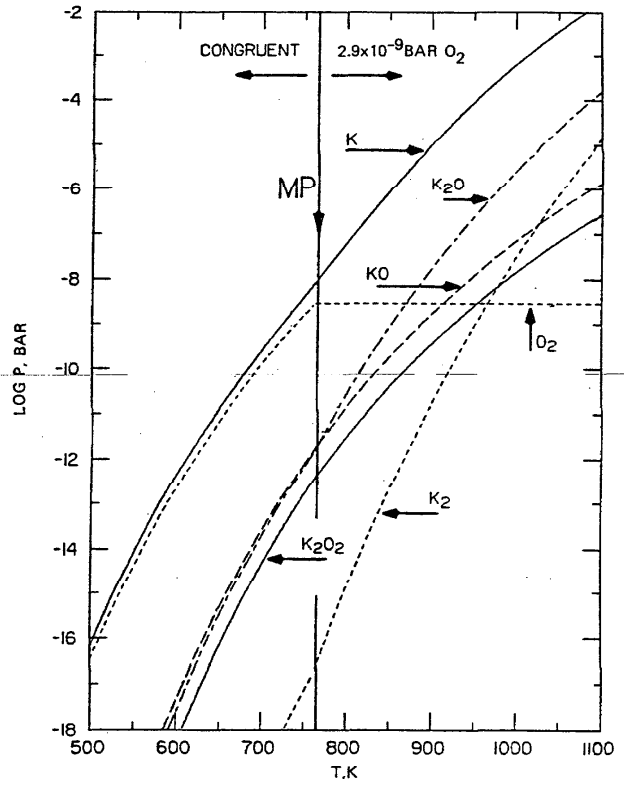

FIG. 10. Congruent vaporization of solid K_2O_2 and vaporization of liquid K_2O_2 in 2.9×10^{-9} bar O_2.

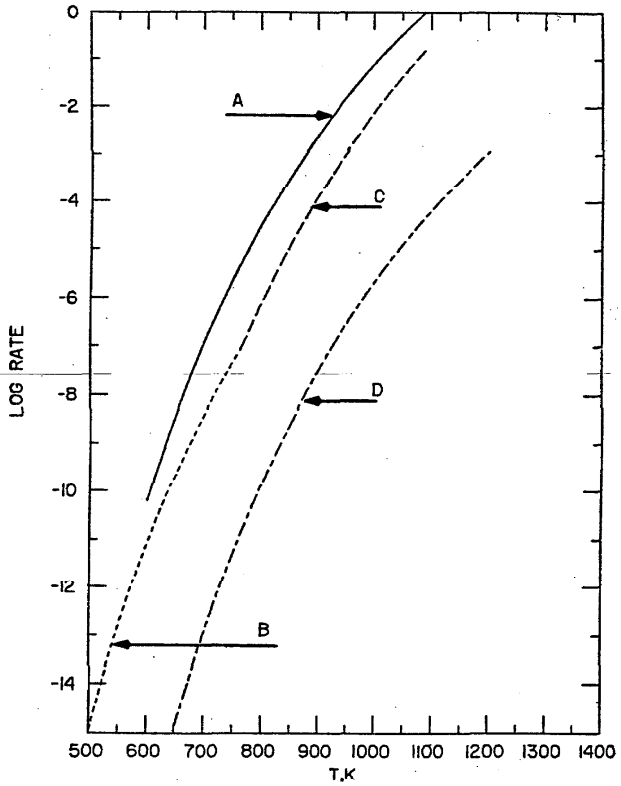

FIG. 12. Potassium oxide maximum vaporization rates. A—K_2O in 10^{-15} bar O_2; B—Congruent vaporization of solid K_2O_2; C—Liquid K_2O_2 in 2.9×10^{-9} bar O_2; D—KO_2 in 0.2 bar O_2. Rate units—g cm^{-2} s^{-1}.

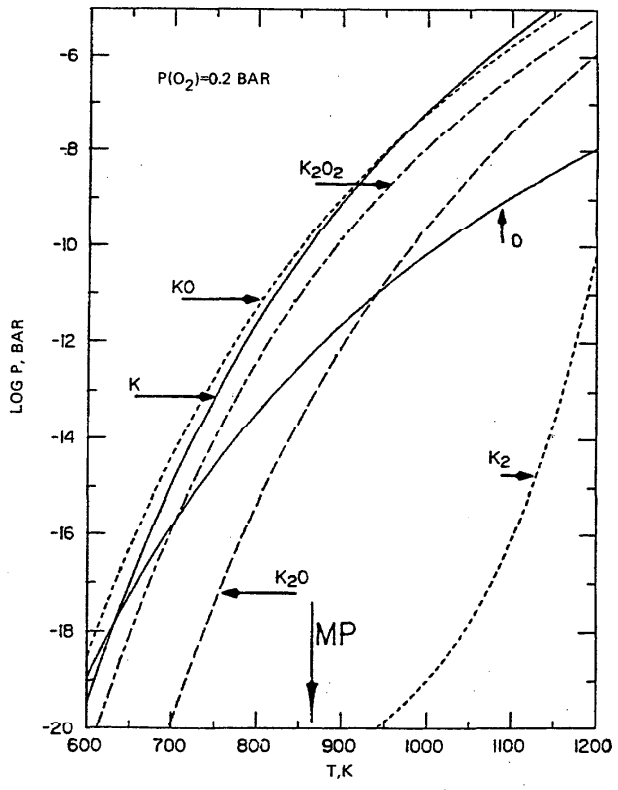

FIG. 11. KO_2 vaporization in 0.2 bar O_2.

vaporizing liquid composition is slightly more potassium-rich than K_2O_2. Since congruent vaporization of K_2O_2 liquid is thus physically unrealistic, the partial pressures of species in equilibrium with liquid K_2O_2 shown in Fig. 10 were calculated using the O_2 pressure found for the congruently vaporizing solid at its melting temperature. Since the liquid composition changes with time under these conditions, the calculated partial pressures apply only for initial vaporization conditions. These comments also apply to the vaporizations of liquid Rb_2O_2 and Cs_2O_2 under neutral conditions discussed below. The partial pressures of species in equilibrium with condensed KO_2 in 0.2 bar of O_2 are shown in Fig. 11, and maximum mass loss rates for potassium oxides under various conditions are shown in Fig. 12.

d. Rb–O System

Partial pressures of species in equilibrium with Rb_2O at an O_2 pressure of 10^{-15} bar, for which Rb_2O is the stable solid phase above 500 K, are shown in Fig. 13. The partial pressures of species calculated for the congruent vaporization of solid Rb_2O_2 are shown in Fig. 14. Since the congruently vaporizing liquid composition is not known, the partial pressures over liquid Rb_2O_2 shown in this figure were calculated for initial vaporization conditions at the oxygen potential of the congruently vaporizing solid at the melting temperature. Figure 15 shows the calculated partial pressure of species in equilibrium with RbO_2 at an oxygen partial pres-

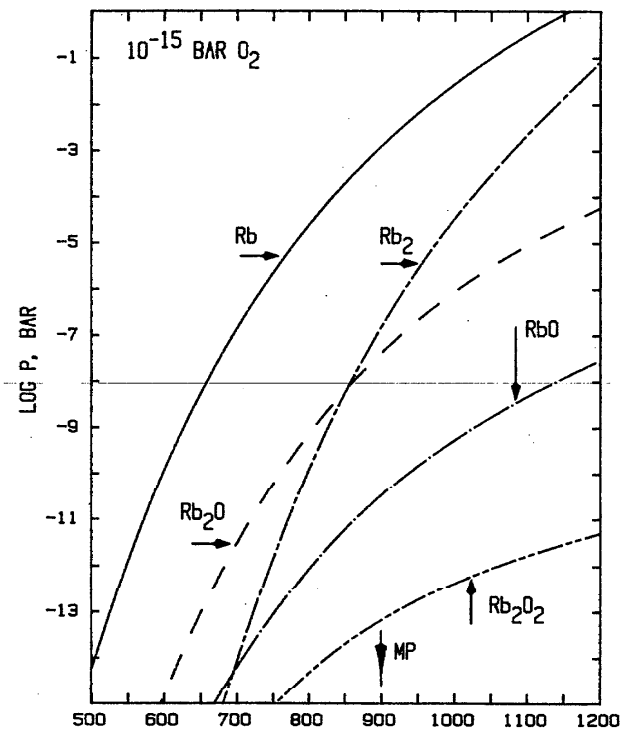

FIG. 13. Rb_2O vaporization in 10^{-15} bar O_2.

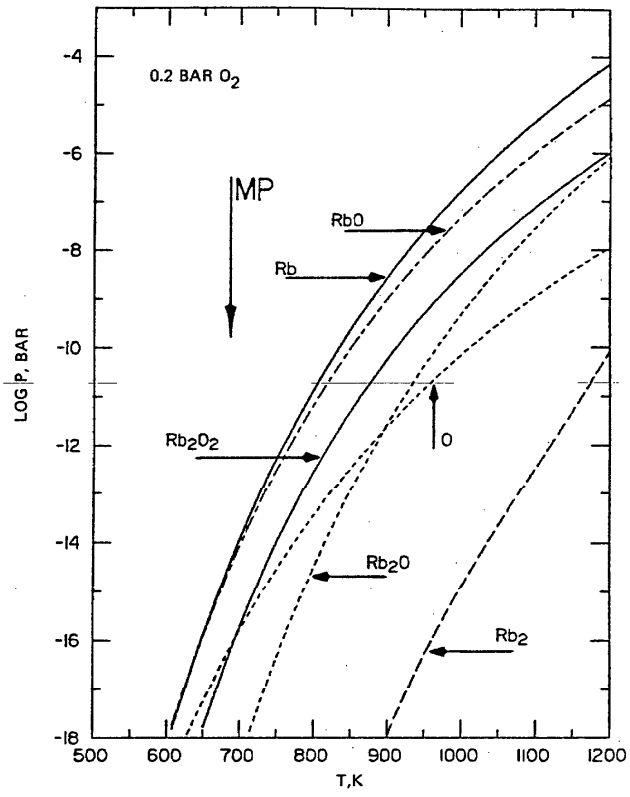

FIG. 15. RbO_2 vaporization in 0.2 bar O_2.

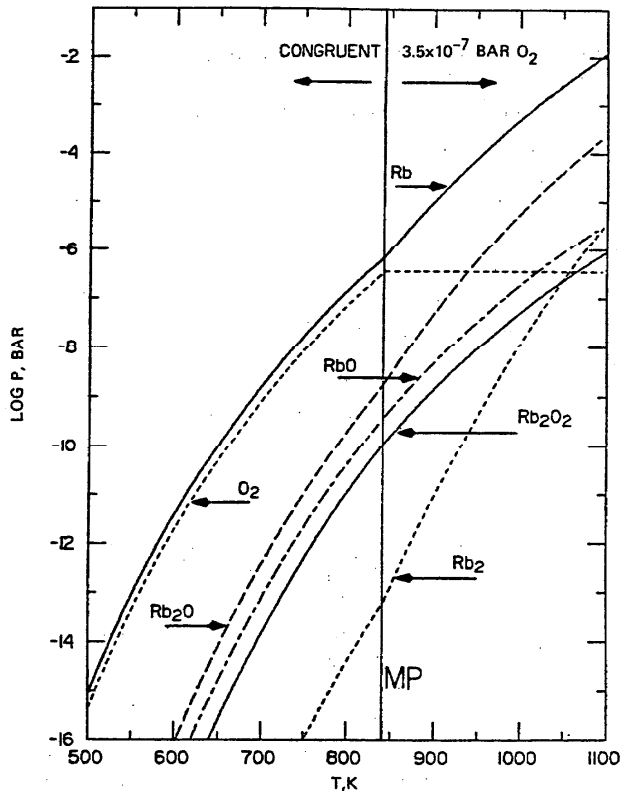

FIG. 14. Congruent vaporization of solid Rb_2O_2 and vaporization of liquid Rb_2O_2 in 3.5×10^{-7} bar O_2.

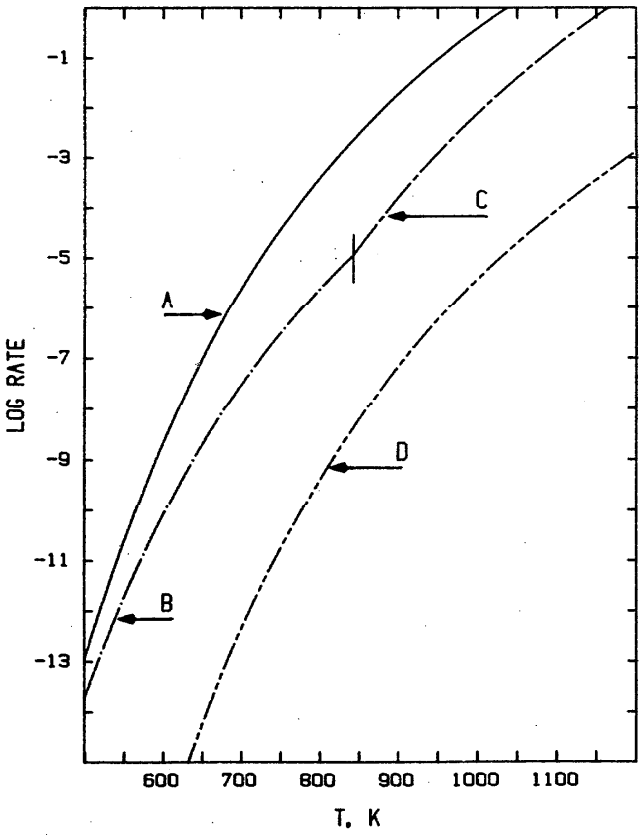

FIG. 16. Rubidium oxide maximum vaporization rates. A—Rb_2O in 10^{-15} bar O_2; B—Congruent vaporization of solid Rb_2O_2; C—Rb_2O_2 in 3.5×10^{-7} bar O_2; RbO_2 in 0.2 bar O_2. Rate units—g cm^{-2} s^{-1}.

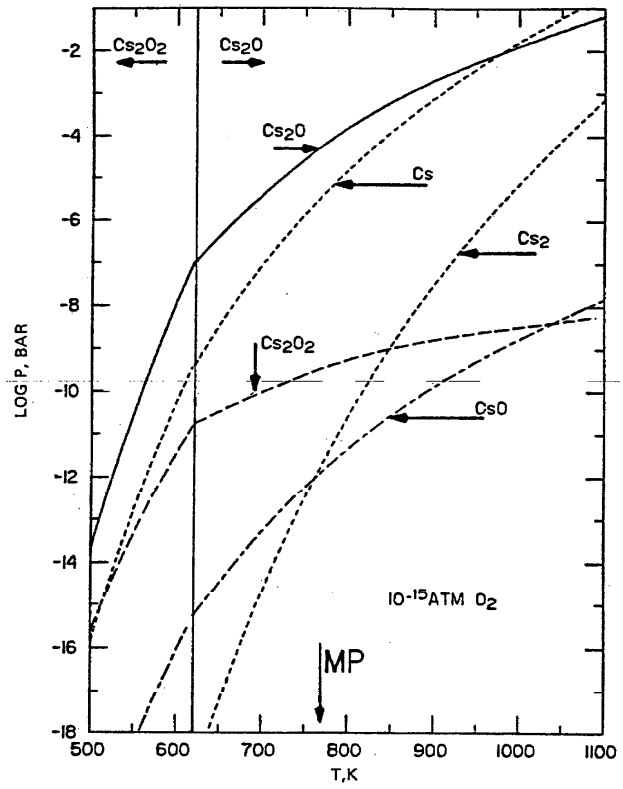

FIG. 17. Vaporization of cesium oxides in 10^{-15} bar O_2. The condensed phases are Cs_2O_2 below 620 K and Cs_2O above this temperature.

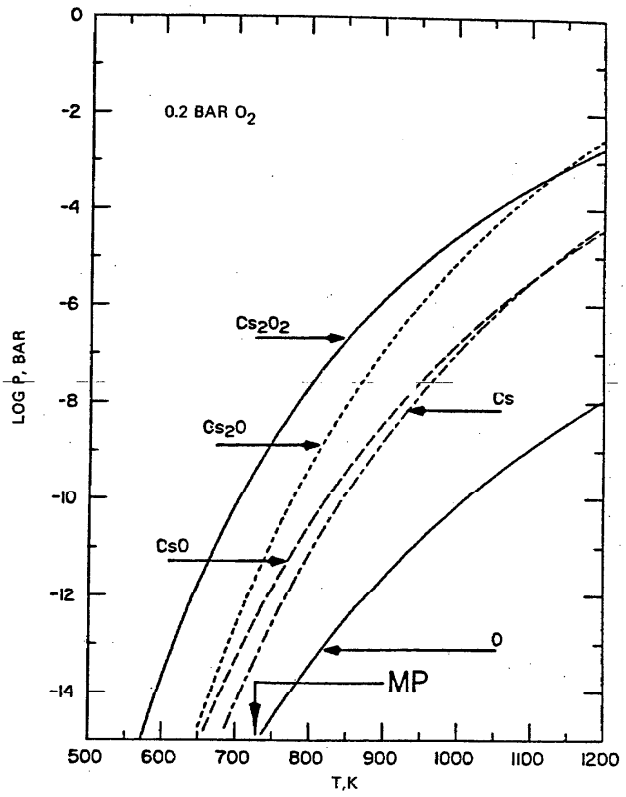

FIG. 19. CsO_2 vaporization in 0.2 bar O_2.

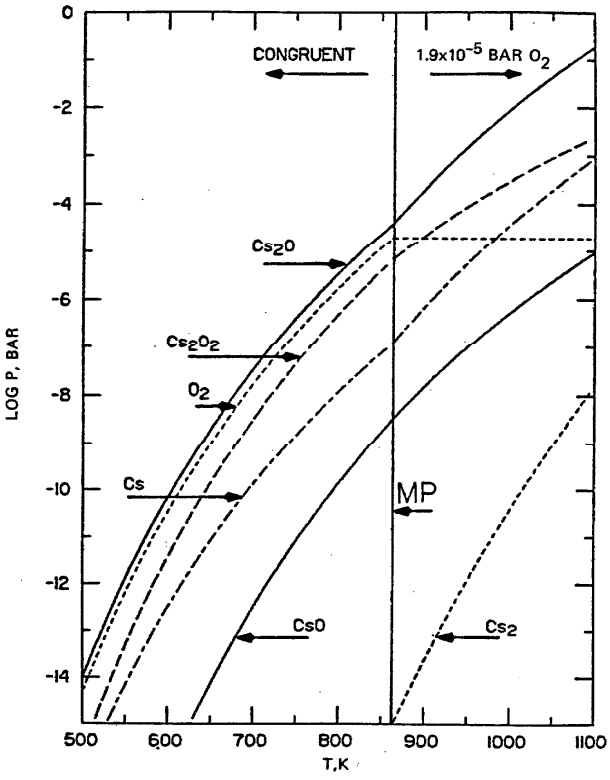

FIG. 18. Congruent vaporization of solid Cs_2O_2 and vaporization of liquid Cs_2O_2 in 1.9×10^{-5} bar O_2.

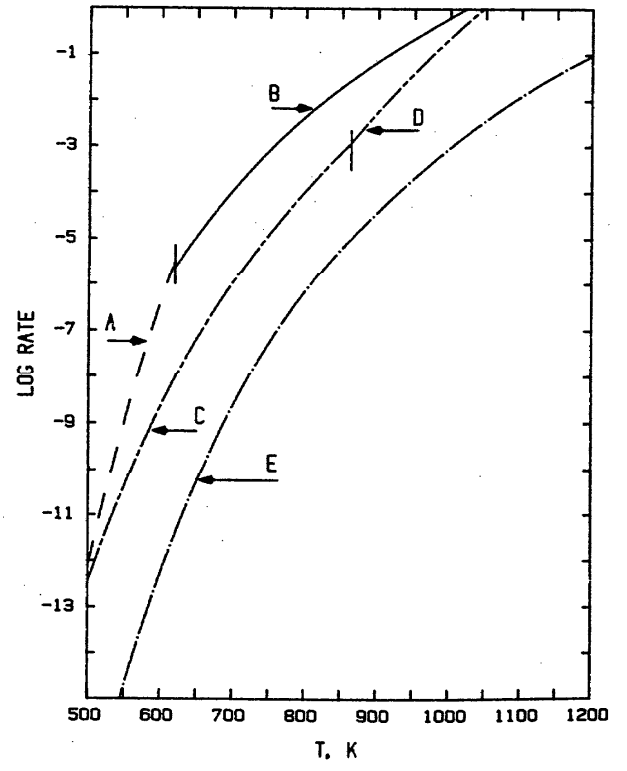

FIG. 20. Cesium oxide maximum vaporization rates. A—Cs_2O_2 in 10^{-15} bar O_2; B—Cs_2O in 10^{-15} bar O_2; C—Congruent vaporization of solid Cs_2O_2; D—Vaporization of liquid Cs_2O_2 in 1.9×10^{-5} bar O_2; E—CsO_2 in 0.2 bar O_2. Rate units—g cm^{-2} s^{-1}.

sure of 0.2 bar. Calculated maximum mass loss rates for these vaporization conditions are shown in Fig. 16.

e. Cs–O System

At an oxygen pressure of 10^{-15} bar, Cs_2O_2 is the stable solid phase below about 620 K, and Cs_2O is stable from this temperature to its melting point. Figure 17 shows the partial pressures of species in equilibrium with Cs_2O under these conditions. The partial pressures of species in equilibrium with congruently vaporizing solid Cs_2O_2 are shown in Fig. 18. Since the congruently vaporizing liquid composition is not known, partial pressures of species in equilibrium with liquid Cs_2O_2 shown in this figure were calculated for initial vaporization conditions at the oxygen potential of the congruently vaporizing solid at its melting temperature. Figure 19 shows the partial pressures calculated for vaporization of CsO_2 in 0.2 bar of O_2. Calculated maximum mass loss rates for the above conditions are shown in Fig. 20.

4. Acknowledgments

We thank Leo Brewer for his advice and constructive comments on the manuscript. Financial support for this work has come from the Office of Standard Reference Data of the National Bureau of Standards under Grant No. NB80NADA1063.

5. References

[1]L. Brewer, Chem. Rev. **52**, 1 (1953).
[2]J. P. Coughlin, U. S. Bur. Mines Bull. **542** (1954).
[3]K. K. Kelley, U. S. Bur. Mines Bull. **584** (1960).
[4]H. L. Schick, *Thermodynamics of Certain Refractory Compounds* (Academic, New York, 1960), Vols. 1 and 2.
[5]R. J. Ackermann and R. J. Thorn, *Progress in Ceramic Science* (Pergamon, New York, 1961), Vol. 1, p. 39.
[6]L. Brewer and G. Rosenblatt, Chem. Rev. **61**, 257 (1961).
[7]L. Brewer and G. M. Rosenblatt, *Advances in High Temperature Chemistry* (Academic, New York, 1969), Vol. 2, p. 1.
[8]K. K. Kelley and E. G. King, U. S. Bur. Mines Bull. **592** (1961).
[9]M. Olette, and M. I. Ancey-Moret, Rev. Metall. (Paris) **60**, 569 (1963).
[10]C. E. Wicks and F. E. Block, U. S. Bur. Mines Bull. **605** (1963).
[11]D. D.Wagman, W. H. Evans, V. B. Parker, I. Halow, S. M. Bailly, and R. H. Schumm, Natl. Bur. Stand. (U. S.) Tech. Note **270-3** (1968).
[12]D. D. Wagman, W. H. Evans, V. B. Parker, I. Halow, S. M. Bailly, and R. H. Schumm, Natl. Bur. Stand. (U. S.) Tech. Note **270-4** (1969).
[13]V. B. Parker, D. D. Wagman, and W. H. Evans, Natl. Bur. Stand. (U. S.) Tech. Note **270-6** (1971).
[14]D. D. Wagman, W.H. Evans, V. B. Parker, I. Halow, S. M. Bailly, R. H. Schumm, and K. L. Churney, Natl. Bur. Stand. (U. S.) Tech. Note **270-5** (1971).
[15]R. H. Schumm, D. D. Wagman, S. M. Bailly, W. H. Evans, and V. B. Parker, Natl. Bur. Stand. (U. S.) Tech. Note **270-7** (1973).
[16]D. D. Wagman, W. H. Evans, V. B. Parker, R. H. Schumm, and R. L. Nuttall, Natl. Bur. Stand. (U. S.) Tech. Note **270-8** (1981).
[17]JANAF Thermochemical Tables, 2nd ed. edited by D. R. Stull, *et al.*, NSRDS-NBS 37 (U.S. GPO, Washington, D.C., 1971). Individual table supplements to this reference are identified by the date of their issue. The published collections of supplementary tables are referenced separately. JANAF data not contained in the 1971 compendium or the collected supplements [74JAN, 75JAN, 78JAN, 82JAN] are referenced as dated supplements to the 1971 work.
[18]M. W. Chase *et al.*, JANAF Thermochemical Tables, 1974 Supplement, J. Phys. Chem. Ref. Data **3**, 311 (1974).
[19]M. W. Chase *et al.*, JANAF Thermochemical Tables, 1975 Supplement, J. Phys. Chem. Ref. Data **4**, 1 (1975).
[20]M. W. Chase, Jr. *et al.*, JANAF Thermochemical Tables, 1978 Supplement, J. Phys. Chem. Ref. Data **7**, 793 (1978).
[21]M. W. Chase, Jr. *et al.*, JANAF Thermochemical Tables, 1982 Supplement, J. Phys. Chem. Ref. Data **11**, 695 (1982).
[22]I. Barin and O. Knacke, *Thermochemical Properties of Inorganic Substances* (Springer, Berlin, 1973); Supplement (1977).
[23]G. V. Samsonov, *The Oxide Handbook* (English translation), (IFI/Plenum, New York, 1973).
[24]G. V. Samsonov *et al.*, *Physiocochemical Properties of Oxides: Handbook*, 2nd ed. (Metallurgiya, Moscow, USSR, 1978).
[25]V. P. Glushko, L. V. Gurvich, G. A. Bergman, I. V. Veitz, V. A. Medvedev, G. A. Khachkuruzov, and V. S. Yungman, *Thermodynamic Data for Individual Substances*, Vol. 1 (1978): The elements O, H, F, Cl, Br, I, He, Ne, Ar, Kr, Xe, Rn, S, N, and P and their compounds; Volume 2 (1979): The elements C, Si, Ge, Sn, and Pb and their compounds; Volume 3 (1981): The elements B, Al, Ga, In, Tl, Be, Mg, Ca, Sr, and Ba and their compounds. High Temperature Institute, State Institute of Applied Chemistry, National Academy of Sciences of the U.S.S.R., Moscow. (The volumes of this series are each in two separately bound parts: the text in Book 1, and tables of thermodynamic properties in Book 2.)
[26]V. P. Glushko *et al.*, *Thermal Constants of Materials, Handbook, No. 10: Lithium, Sodium, Potassium, Rubidium, Cesium, and Francium*, Part 1 (1981), Tables of Accepted Values: Li, Na; Part 2 (1981), Tables of Accepted Values: K, Rb, Cs, and Fr; Part 3, Literature Citations, Appendices, References, and Index, Akad. Nauk SSSR, Inst. Vys. Temp., Moscow, USSR.
[27]L. B. Pankratz, U. S. Bur. Mines Bull. **672** (1982).
[28]J. B. Pedley and E. M. Marshal, J. Phys. Chem. Ref. Data **12**, 967 (1983).
[29]E. S. Rittner, J. Chem. Phys. **19**, 1030 (1951).
[30]D. L. Hildenbrand, J. Electrochem. Soc. **126**, 1396 (1979).
[31]CODATA Recommended Key Values for Thermodynamics, 1977, J. Chem. Thermodyn. **10**, 903 (1978).
[32]K. S. Pitzer and L. Brewer, J. Phys. Chem. Ref. Data **8**, 917 (1979).
[33]Commission on Atomic Weights, Inorganic Chemistry Division of IUPAC, Pure Appl. Chem. **47**, 75 (1976).
[34]R. P. Elliott, *Constitution of Binary Alloys*, Supplement Number 1 (McGraw–Hill, New York, 1965).
[35]N.-G. Vannerberg, Prog. Inorg. Chem. **4**, 125 (1962).
[36]L. A. D'Orazio and R. H. Wood, J. Phys. Chem. **69**, 2550 (1965).
[37]R. H. Snow, Illinois Institute of Technology Research Institute, Chicago, Report No. AD626590, 1965.
[38]I. I. Vol'nov, S. A. Tokareva,V. N. Belevskii, and V. I. Klimanov, Izv. Akad. Nauk SSSR, Ser. Khim. **1967**, 1411.
[39]L. Malaspina, R. Gigli, and V. Piacente, Gazz. Chim. Ital. **101**, 197 (1971).
[40]A. S. Dworkin and M. A. Bredig, J. Phys. Chem. **72**, 1277 (1968).
[41]T. Tanifuji and S. Nasu, J. Nucl. Mater. **78**, 422 (1978).
[42]A. E. van Arkel, E. A. Flood, and N. F. H. Bright, Can. J. Chem. **31**, 1009 (1953).
[43]L. Brewer and J. L. Margrave, J. Phys. Chem. **59**, 421 (1955).
[44]G. Papin, M. Michaud, and R. Bouaziz, C. R. Acad. Sci. Ser. C **268**, 1691 (1969).
[45]M. Akiyama, K. Ando, and Y. Oishi, J. Nucl. Sci. Technol. **17**, 154 (1980).
[46]M. S. Ortman and E. M. Larsen, *Studies on Tritium Breeders for Fusion Reactors, I. The Preparation, Characterization, and Melting Point of Lithium Oxide*, UWFDM-449, University of Wisconsin, Madison, Wisconsin, August, 1982.
[47]A. J. Leffler and N. M. Wiederhorn, J. Phys. Chem. **68**, 2882 (1964).
[48]R. Hultgren, P. D. Desai, D. T. Hawkins, M. Gleiser, K. K. Kelley, and D. D. Wagman, *Selected Values of the Thermodynamic Properties of the Elements* (American Society for Metals, Metals Park, Ohio, 1973).
[49]D. R. Fredrickson and M. G. Chasanov, J. Chem. Thermodyn. **6**, 629 (1974).
[50]D. F. Fredrickson and M. G. Chasanov, J. Chem. Thermodyn. **5**, 485 (1973).
[51]R. T. Grimley and J. L. Margrave, J. Phys. Chem. **64**, 1763 (1960).
[52]J. L. Henry, S. A. O'Hare, and M. P. Krug, Albany Research Center, Albany, Oregon, Report No. USBM-1532, 1971.
[53]R. Bouaziz, G. Papin, and A. Rollet, C. R. Acad. Sci. **1262**, 1051 (1966).
[54]P. A. G. O'Hare, J. Chem. Phys. **56**, 4513 (1972).
[55]P. Gross and T. L. Wilson, J. Chem. Soc. A **1970**, 1913.
[56]F. A. Shunk, *Constitution of Binary Alloys*, Supplement Number 2 (McGraw–Hill, New York, 1969).

[57]H. J. Byker, I. Eliezer, R. C. Howald, and T. C. Ehlert, High Temp. Sci. **11**, 153 (1979).
[58]A. W. Petrocelli, Ph.D. thesis (University of Rhode Island, 1960).
[59]N. Eliezer, R. A. Howald, M. Marinkovic, and I. Eliezer, J. Phys. Chem. **82**, 1021 (1978).
[60]F. Natola and P. Touzain, Can. J. Chem. **48**, 1955 (1970).
[61]L. L. Simmons, L. Lowden, and T. C. Ehlert, J. Phys. Chem. **81**, 706 (1977).
[62]E. Rengade, Ann. Chim. Phys. **14**, 540 (1908).
[63]J. F. Riley, Ph.D. thesis (University of Rhode Island, 1969); Diss. Abstr. **30**, 598B (1969).
[64]I. A. Kazarnovskii and S. I. Raikhshtein, Zh. Fiz. Khim. **21**, 245 (1947).
[65]A. Simon. Struct. Bonding (Berlin) **36**, 81 (1979).
[6]I. E. Paukov, F. S. Rakhmenkulov, M. S. Dobrolyubova, and A. B. Tsentsiper, Izv. Akad. Nauk SSSR, Ser. Khim. **1970**, 2135.
[67]M. Centnersziver and M. Blumenthal, Bull. Int. Acad. Pol. Sci. Lett. Cl. Sci. Math. Nat. Ser. A **1933**, 494 (1933).
[68]D. L. Kraus and A. W. Petrocelli, J. Phys. Chem. **66**, 1225 (1962).
[69]R. de Forcrand, C. R. Acad. Sci. **158**, 991 (1914).
[70]C. F. Knights and B. A. Phillips, J. Nucl. Mater. **84**, 196 (1979).
[71]R. G. Behrens, H. O. Woodrow, and S. Aronson, J. Chem. Thermodyn. **9**, 1044 (1977).
[72]H. E. Flotow and D. W. Osborne, J. Chem. Thermodyn. **6**, 135 (1974).
[73]S. P. Berardinelli, Sr. and D. L. Kraus, Inorg. Chem. **13**, 189 (1974).
[74]K. P. Huber and G. Herzberg, *Constants of Diatomic Molecules* (Van Nostrand, New York, 1979).
[75]M. J. McEwan and L. F. Phillips, Trans. Faraday Soc. **62**, 1717 (1966).
[76]D. L. Hildenbrand and E. Murad, J. Chem. Phys. **53**, 3403 (1970).
[77]R. C. Feber and C. C. Herrick, Los Alamos Scientific Laboratory Report No. LA-3597, 1966.
[78]D. D. Konowalow and M. L. Olson, J. Chem. Phys. **71**, 450 (1979).
[79]V. Piacente, G. Bardi, and L. Malaspina, J. Chem. Thermodyn. **5**, 219 (1973).
[80]D. White, K. S. Seshadri, D. F. Dever, D. E. Mann, and M. J. Linevsky, J. Chem. Phys. **39**, 2463 (1963).
[81]D. L. Hildenbrand, W. F. Hall, and N. D. Potter, J. Chem. Phys. **39**, 296 (1963).
[82]J. H. Norman and P. Winchell, General Atomic Division of General Dynamics Report No. GA-7597, 1967.
[83]Y. Ikeda, H. Ito, G. Matsumoto, and S. Nasu, Shitsuryo Bunseki **27**, 263 (1979).
[84]A. V. Gusarov, L. N. Gorokhov, and A. G. Efimova, Teplofiz. Vys. Temp. **5**, 584 (1967); English translation: High Temp. (USSR) **5**, 524 (1967).
[85]L. N. Gorokhov "High Temperature Technology," in *Proceedings of the Third International Symposium, Asilomar, California, 1967* (Butterworths, London, 1969), p. 647.
[86]L. Andrews, J. Chem. Phys. **50**, 4288 (1969).
[87]L. Andrews, J. Phys. Chem. **73**, 3922 (1969).
[88]L. Andrews, J. Chem. Phys. **54**, 4935 (1971).
[89]L. Andrews, J.-T. Hwang, and C. Trindle, J. Phys. Chem. **77**, 1065 (1973).
[90]J. H. Yates and R. M. Pitzer, J. Chem. Phys. **66**, 3592 (1977).
[91]M. Yoshimine, J. Chem. Phys. **57**, 1108 (1972).
[92]C. H. Wu, H. Kudo, and H. R. Ihle, J. Chem. Phys. **70**, 1815 (1979).
[93]H. Kudo, C. H. Wu, and H. R. Ihle, J. Nucl. Mater. **78**, 380 (1978).
[94]H. Kimura, M. Asano, and H. Kubo, J. Nucl. Mater. **92**, 221 (1980).
[95]C. H. Wu, J. Chem. Phys. **65**, 3181 (1976).
[96]K. Kimoto, I. Nishida, H. Takahashi, and H. Kato, Jpn. J. Appl. Phys. **19**, 1821 (1980).
[97]W. Gerber and E. Schumacher, J. Chem. Phys. **69**, 1692 (1978).
[98]J. Kendrick and I. H. Hillier, Mol. Phys. **33**, 635 (1977).
[99]H.-O. Beckmann, J. Koutecky, P. Botschwina, and W. Meyer, Chem. Phys. Lett. **67**, 119 (1979).
[100]H.-O. Beckmann, J. Koutecky, and V. Bonacic-Koutecky, J. Chem. Phys. **72**, 5182 (1980).
[101]E. Rengade, Ann. Chim. Phys. **11**, 348 (1907).
[102]J. Berkowitz, W. A. Chupka, G. D. Blue, and J. L. Margrave, J. Phys. Chem. **63**, 644 (1959).
[103]D. Beruto, L. Barco, and A. Passerone, "Refractory Oxides: High Temperature Solid-Gas and Solid-Liquid Behavior," in *Oxides and Oxide Films*, edited by A. K. Vijh (Dekker, New York, 1981), Vol. 6, pp. 1–84.
[104]E. T. Turkdogan, *Physical Chemistry of High Temperature Technology* (Academic, New York, 1980), pp. 230–234.
[105]D. L. Hildenbrand, J. Chem. Phys. **57**, 4556 (1972).
[106]G. K. Johnson, R. T. Grow, and W. N. Hubbard, J. Chem. Thermodyn. **7**, 781 (1975).
[107]T. C. Ehlert, High Temp. Sci. **9**, 237 (1977).
[108]J. Hilsenrath, C. G. Messina, and W. H. Evans, Air Force Weapons Laboratory Report No. TDR-64-44, Kirtland Air Force Base, New Mexico, 1964.
[109]D. L. Martin, Can. J. Phys. **48**, 1327 (1970).
[110]J. L. Settle, G. K. Johnson, and W. N. Hubbard, J. Chem. Thermodyn. **6**, 263 (1974).
[111]P. J. Touzain, J. Therm. Anal. **9**, 441 (1976).
[112]P. A. G. O'Hare and A. C. Wahl, J. Phys. Chem. **56**, 4516 (1972).
[113]R. T. Spiker, Jr. and L. Andrews, J. Chem. Phys. **58**, 713 (1973).
[114]A. Dalgarno, Adv. Phys. **11**, 281 (1962).
[115]C. E. Moore, Natl. Bur. Stand. (U. S.) Circ. **467** (1958).
[116]L. Andrews and R. R. Smardzewski, J. Chem. Phys. **58**, 2258 (1973).
[117]R. R. Smardzewski and L. Andrews, J. Chem. Phys. **57**, 1327 (1972).
[118]R. R. Smardzewski and L. Andrews, J. Chem. Phys. **77**, 801 (1973).
[119]S. M. Tolmachev, E. Z. Zasorin, and N. G. Rambidi, Zh. Strukt. Khim. **10**, 541 (1969). English translation: J. Struct. Chem. (USSR) **10**, 449 (1969).